

Structure prediction and structure determination of solids via investigation of their energy landscapes

J. C. Schön

Max-Planck-Institut für Festkörperforschung
70569 Stuttgart

Funding: DFG

Together with: Dr. H. Putz, Dr. M. Wevers, M. Sci. Z. Cancarevic, Prof. Dr. M. Jansen

Comments

- Since the viewgraphs by themselves are not overly helpful, some short comments and references are included after each viewgraph.
- A general overview over the energy landscape approach to structure prediction can be found in [1] and [2, 3]

A short (ideosyncratic) history of structure prediction and determination in extended solids using energy landscape methods

- Physics (long ago):
 - $H = H_{ion} + H_{elec} + H_{ion-elec}$
→ $H_{eff}(\vec{R}_{ion})$ in electronic ground state (BOA)
 - $E(\vec{R}_{ion}) = \text{minimum}$ yields structure \vec{R}_{ion}^0 bei $T = 0$
 - \vec{R}_{ion}^0 produces measurement data
- Long-standing questions
 - Can one find \vec{R}_{ion}^0 ? (global optimization problem)
i.e.: **Structure prediction**
 - Given incomplete measurement data, can one find \vec{R}_{ion}^0 with help from $H_{eff}(\vec{R}_{ion})$?
i.e.: **Structure determination**
 - Given parameters of synthesis route, can one predict the outcome? (dual problem: given desired outcome, can one design synthesis route?)
i.e.: **Structure simulation**
- Global optimization methods, e.g. GenAlg (Holland 1975) or SimAnn (Kirkpatrick et al. 1983, Cerny 1985)

- Structure determination
 - RMC (McGreevy et al. 1988) using SimAnn with cost functions (powder data + constraints) for amorphous systems structure suggestions
 - Measurement → cell constants + cell content
 - ”Energy”-based cost functions + keep cell constants fixed + global optimization procedure → structure (Pannetier et al. 1990, Freeman et al. 1993)
 - Pareto optimization
 - * ”Powder data” + ”energy” like terms using global optimization procedure → structure (Deem et al. 1989)
 - * Powder diffractogram + energy function using global optimization procedure → structure (1999, Coelho 2000, Lanning et al. 2000)
- Structure prediction
 - Structure ”guesses” + ab initio energy (Liu et al. 1990)
 - Free cell, free composition, free charges + potential energy as cost function + global optimization (since 1993)
 - Primary building units (1999)
 - Secondary building units (Mellot-Draznieks et al. 2000)
- Structure simulation
 - Quenching from the melt (since about 1980; more realistic systems since about 1990)
 - Freezing from the melt (simple liquids since about 1990)
 - Sol-gel processes (since about 1980; more realistic systems since about 2000)

Comments

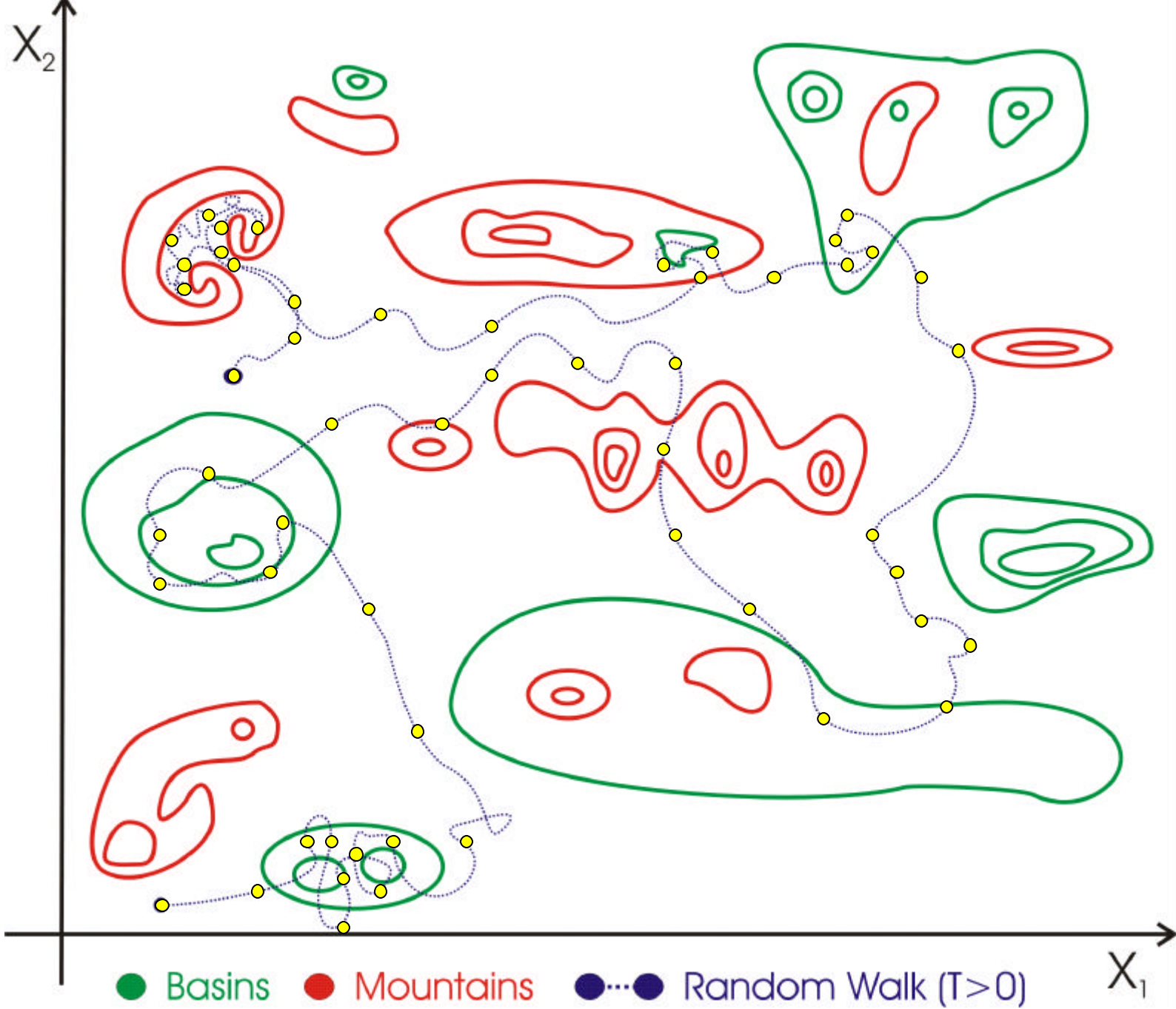
- Physics
 - First step is the separation of electronic and ionic degrees of freedom, followed by the integration of the electronic degrees of freedom (i.e. solving the Schrödinger equation for arbitrary but fixed atom positions).
 - Focus on electronic ground state: Born-Oppenheimer approximation; effective Hamiltonian depends only on ionic coordinates \vec{R}_{ion} ; plot of the effective potential energy of the ions results in the Born-Oppenheimer ground state energy surface as function of $3N$ coordinates (for a solid consisting of N ions)
 - At $T = 0$ K, a minimum \vec{R}_{ion}^0 of the effective energy corresponds to a metastable structure
 - X-ray/neutron/electron diffraction measures approximate location of the ionic positions \vec{R}_{ion}^0 , if the structure is "stable" for a long enough time
 - These general aspects are true for the structure of individual molecules, molecular solids, and extended solids. In the following, only reference is being made to extended solids; for molecular solids, proteins, etc., see [2, 3] and references cited therein.
- Clarification of what is meant by "structure prediction", "structure determination", and "structure simulation". Sometimes, "structure determination" is also called "structure solution". Also, in the older literature, work that should be classified as "structure determination" is sometimes advertised as "structure prediction". However, since the knowledge of e.g. the cell coordinates together with the composition massively restricts the range of feasible structures, "prediction" of atom positions when given this information really should be termed "structure determination".
- Genetic algorithms[4] and simulated annealing[5, 6], together with their innumerable variants, are just two very common, moderately efficient but generally applicable, and relatively easy to implement global optimization procedures. For details of these methods, and the description of other alternative methods, see the literature[2, 3]. Note that heuristics can be more efficient than these stochastic methods, if one has enough knowledge about major features of the energy landscape. In the context of the stochastic methods, such landscape information can be used to improve the design of the so-called moveclass (system of neighborhoods of each configuration from which trial candidates are chosen at random) resulting in possibly great improvements in the efficiency of the algorithms.
- From the point of view of optimization, the "energy function" is just a special "cost function" or "objective function"
- The energy landscapes exhibit extremely large numbers of local minima. Thus, exhaustive search + local optimization usually does not work. Not all exploration moves are continuous, i.e., gradient methods are not always applicable

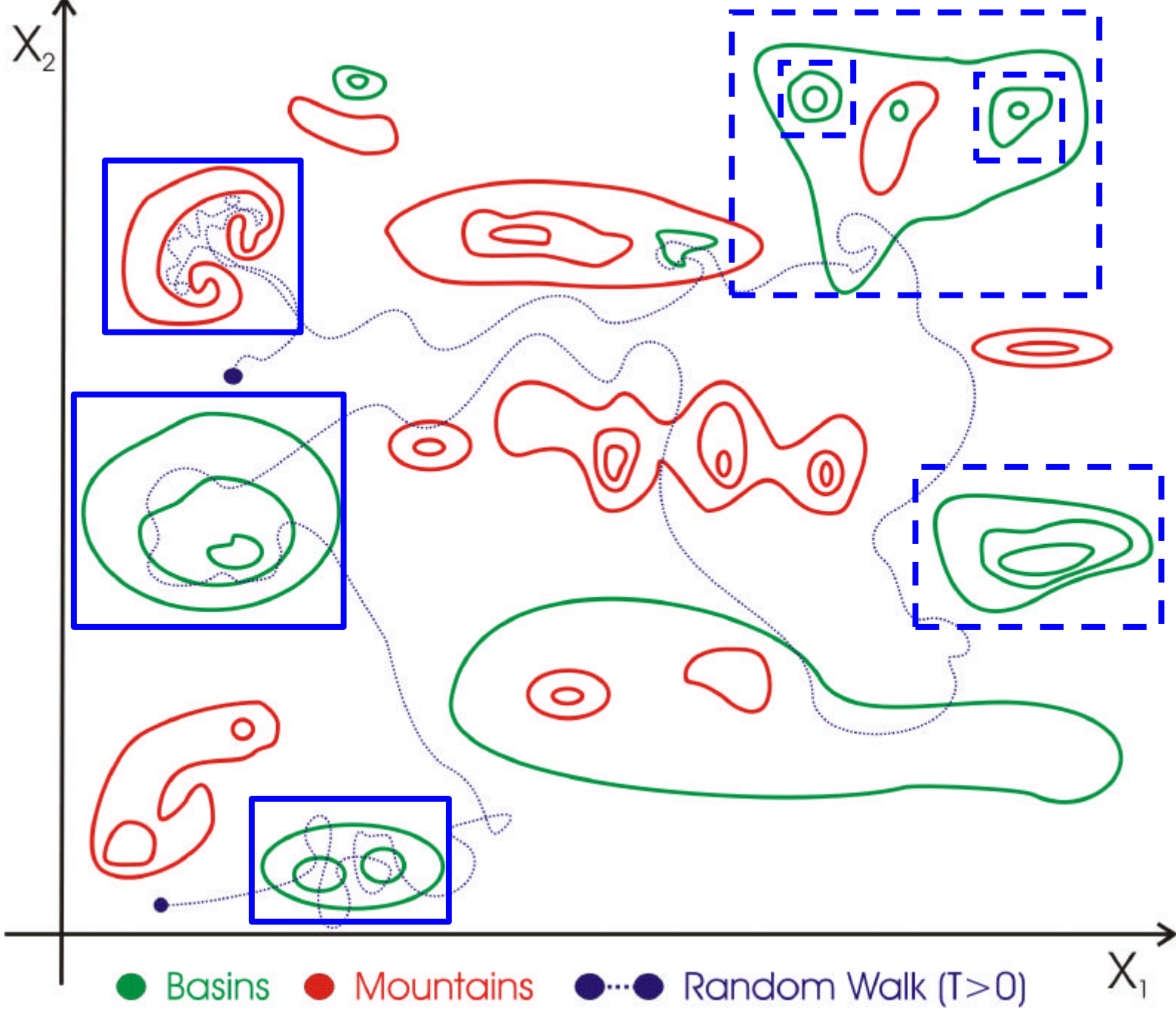
Comments

- Structure determination
 - For RMC, c.f. [7]; for restriction due to measurement input combined with "energy"-based cost functions, c.f. [8, 9]. Note that "chemically inspired" cost functions (e.g. containing bond-valence terms) can often only be used once e.g. cell parameters and composition are fixed. Such non-energy terms tend to be problematic when cells are not given, since the relative weights of the "potential energy"- and e.g. the "bond-valence"-term in the cost function are not known a priori, and thus can easily lead to nonsense results.
 - Pareto optimization denotes the use of cost functions that consist of a sum of two (or more) terms that are independent of each other, and whose relative weights in a cost function are impossible to know a priori (originally used in economic theory, where e.g. job features such as pay, travel time between home and work, and working time compete and are difficult to optimize together). These cost functions can lead to successful structure determinations because they tend to "agree" for "good" structures, i.e., both terms individually have very low values once we are close to chemically and physically "reasonable" atom arrangements, while they eliminate "undesired" structures because these either are energetically unfavorable or clearly disagree with e.g. the powder diffractogram. For references, c.f. [10, 11, 12, 13].
- Structure prediction
 - Very common, popular approach: "Guess" a structure from experience or by searching some database, and follow this step by local optimization of all candidates, preferably on ab-initio level[14]. Nowadays, one can also use systematic generation of structures via "chemical" building principles[15, 16], e.g. by filling dense packings of anions with various cations. However, the number of candidates generated in this fashion grows exponentially or even factorially, making the local optimizations nearly impossible to perform. Trying to cut this plethora of structures back systematically, requires some heuristics which tends to be informed by (chemical) experience (turning the procedure into a high-class "guessing").
 - Our approach consists of two basic steps[17, 1, 2, 3]: global optimizations using a simple empirical potential with free variation of atom positions, cell parameters, charges, and composition (by explicitly adding/removing of atoms), followed by local optimizations on ab initio level.
 - Building units are introduced to a) cut down the number of parameters that need to be optimized, and b) include structures that involve more complex local energy terms than the ones included in the simple potentials usually employed.
 - Primary building units[18, 19, 20]: Fixed spatial arrangements of several atoms that move jointly during the optimization
 - Secondary building units[21, 20]: Fixed spatial arrangements of several atoms, where atoms on the outside (corners) of the building units can merge during the optimization. Thus, the composition is not preserved, even without explicit addition/removal of atoms during the optimization.
- Structure simulation
 - Trying to simulate the full synthesis route is very difficult even for molecular reactions, and nearly impossible for solids.
 - Modeling quenching/cooling from a melt is probably the most "developed" way up to now. Similarly, modeling the sol-gel process is another route that has been investigated at least on a preliminary level.



Figure 1:
Mountain region viewed as an energy landscape.





Comments

- Figures shows 2d-projection of 3N-dimensional landscape
- Blue line shows trajectory of time evolution of a system on the landscape. This applies both to a trajectory of a real system and one simulated in the computer.
- Yellow dots indicate equal time steps, e.g. two dots might be separated in time by one minute (for a real system) or one nanosecond (for a simulated system).
- Measurements correspond to time averages of observables along the trajectory over a time interval (e.g. encompassing 4 minutes)
- Note that the trajectory spends more time in certain regions than in others. In particular, some regions are "explored" rather thoroughly, i.e., one could replace the time average along the trajectory within such a region by a (weighted) average over all states in the region, without making too much of a mistake. If that is feasible, one says that this region of the landscape is "locally ergodic". The regions enclosed in dark blue rectangles are such regions that have been observed along the trajectory shown (e.g. during a Monte Carlo simulation). The dashed rectangles are those that exist, but that have not been found during this particular simulation run. It is clear that a comprehensive study of the landscape requires many such simulation runs.
- Figuratively, the average time needed to explore a region \mathcal{R} sufficiently well is the equilibration time $\tau_{eq}(\mathcal{R})$ of the region. The average time needed to find an exit is the escape time $\tau_{esc}(\mathcal{R})$. For our purposes, we are interested in finding regions of the landscape that equilibrate fast enough, and are also stable enough to have escape times long enough, to permit a measurement (e.g. a diffraction experiment): $\tau_{eq} < t_{obs} < \tau_{esc}$.

Energy landscape concepts

- Definition of landscape

- $\vec{R}_{ion} = (\vec{r}_1, \dots, \vec{r}_{3N})$

- Configuration space $\mathcal{S} = \{\vec{R}_{ion}\}$

- Energy function $E(\vec{R}_{ion}) : R^{3N} \rightarrow R^1$

- (or cost function $C(\vec{R}_{ion})$)

- Add neighborhood relation \rightarrow energy landscape

- Measurements

- $\langle O \rangle_{t_1, t_2} = \frac{1}{t_{obs}} \int_{t_1}^{t_2} O(\vec{r}_I(t), \vec{v}_I(t)) dt$

- $\langle O \rangle_{ens}(\mathcal{R}) = \frac{1}{Z(\mathcal{R})} \sum_{i \in \mathcal{R}} O(i) \exp(E_i/k_B T)$

- $Z(\mathcal{R}) = \sum_{i \in \mathcal{R}} \exp(E_i/k_B T)$

- Local ergodicity

- (Local) ergodicity on the time scale t_{obs}
with accuracy a_M for region \mathcal{R}

- $|\langle O \rangle_{t_{obs}} - \langle O \rangle_{ens}(\mathcal{R})| < a_M$

- $\tau_{eq}(O, \mathcal{R}) < t_{obs} < \tau_{esc}(\mathcal{R})$

Comments

- The definition of a landscape requires three elements: A configuration space of states (or legal solutions of an optimization problem), an energy (or cost) function given as function of the states, and a neighborhood relation (topology). Energy landscapes of atomic configurations usually have "natural" neighborhoods given by the topology of R^{3N} , but for optimization problems we have to explicitly define such a neighborhood relation (called moveclass) which becomes an essential part of the optimization procedure.
- $Z(\mathcal{R})$ is the standard canonical partition function restricted to the locally ergodic region \mathcal{R} .

Landscape concepts

- Landscape simplification

- Locally ergodic regions:

$$\tau_{eq}(\mathcal{R}; O) \ll \tau_{esc}(\mathcal{R}; b_{esc} \ll 1) < \tau_{out}(\mathcal{R}) = \tau_{esc}(\mathcal{R}; b_{esc} \approx 1)$$

- Transition regions:

$$\tau_{out}(\mathcal{R}) < \tau_{eq}(\mathcal{R})$$

- Graph models:

Tree graphs, transition maps, characteristic regions graph

- Useful static features (low temperatures)

- Minima

- Saddle points

- Characteristic regions: Set of all states \vec{x} with the same quench probabilities $P_Q(\vec{x}; \vec{x}_i)$ into local minima \vec{x}_i

- Local densities of states

- Stability of locally ergodic regions

- Generalized barrier:

$$B(\mathcal{R}; T) = B_E + B_S + B_D \propto \ln(\tau_{esc}, \tau_{out})$$

$$B_E \propto \frac{E_{top} - E_{bottom}}{T} - \ln \left(\frac{N_{top}}{N_{bottom}} \right), \quad B_S = \ln \left(\frac{N_{top}}{N_{saddle}} \right),$$

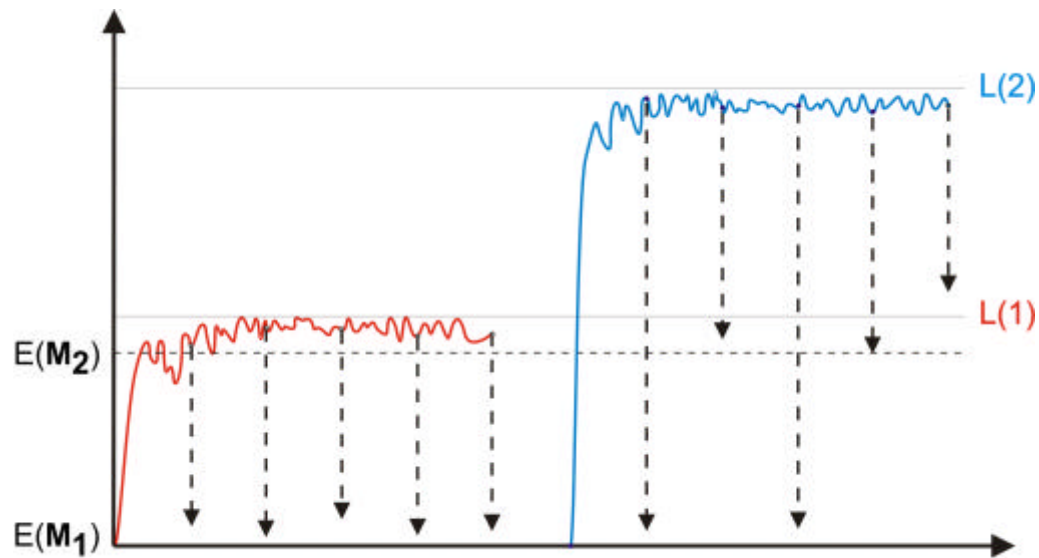
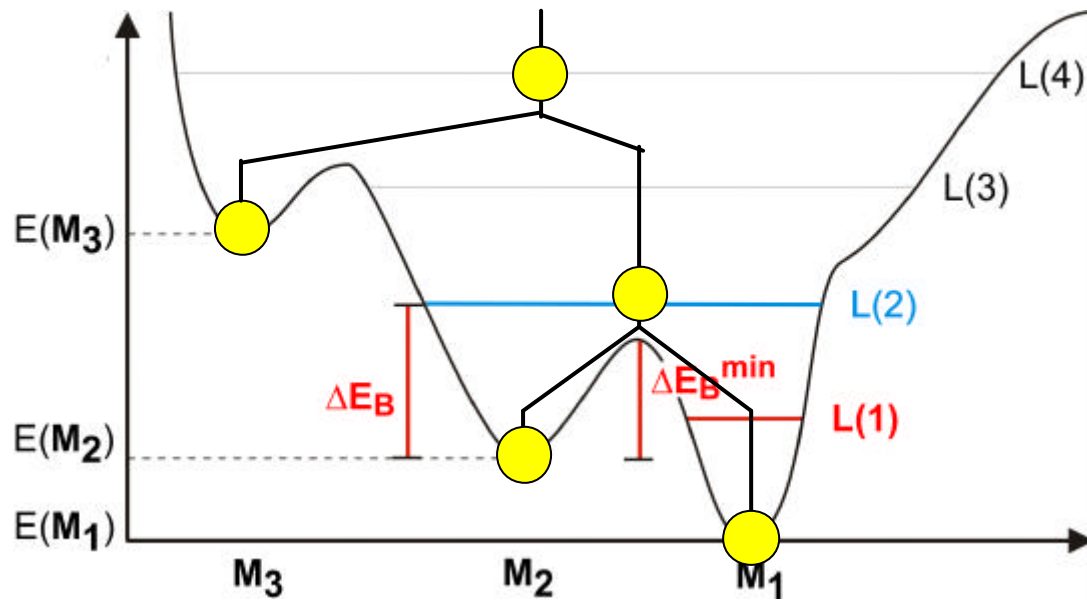
B_D represents labyrinthine aspects

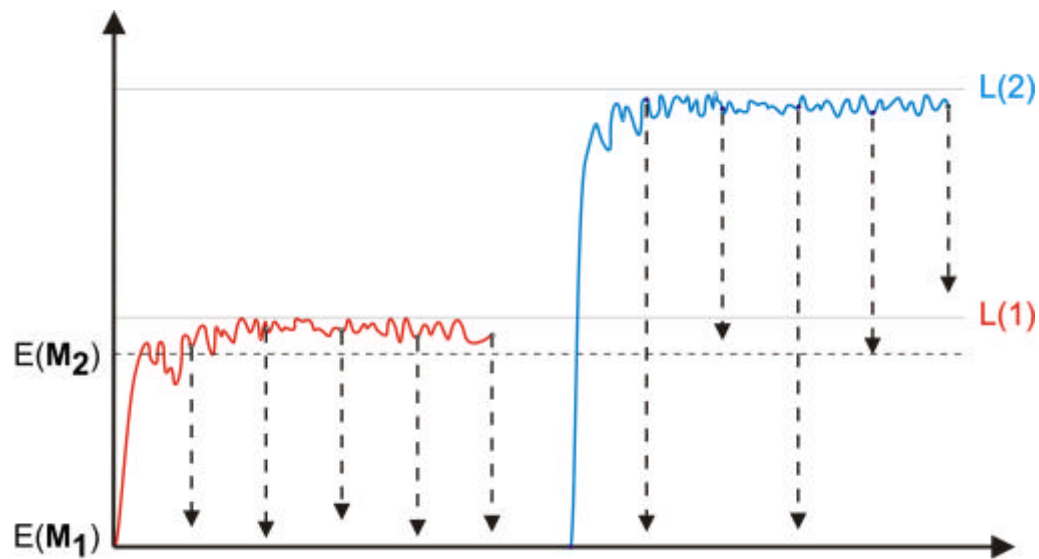
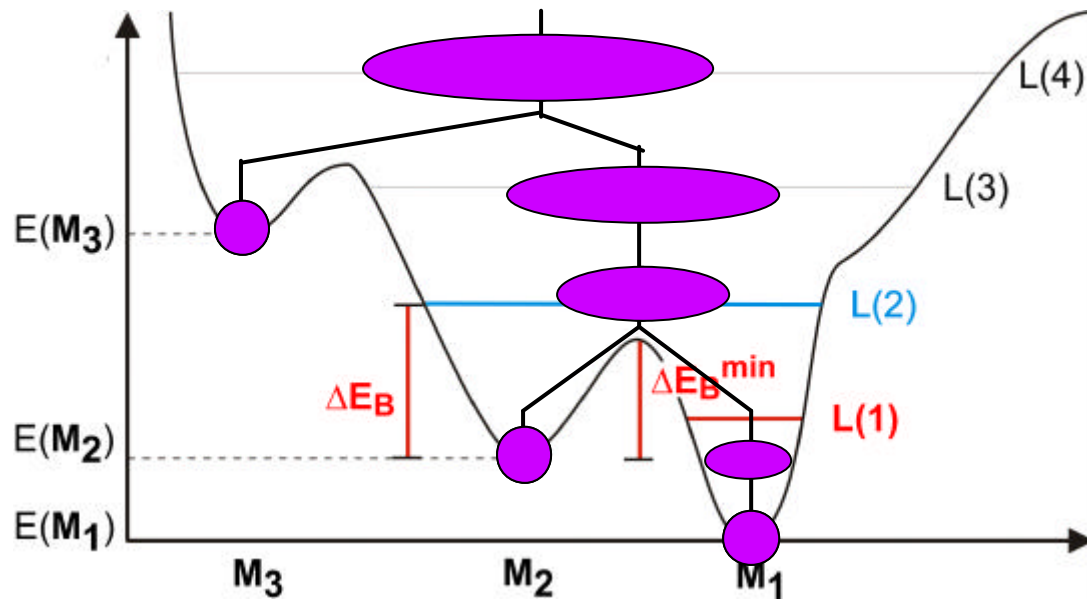
- Time scales $\tau_{esc}, \tau_{out}, \tau_{eq}$ of region \mathcal{R}

- Exit probabilities $p_{exit}(\mathcal{R}_i \rightarrow \mathcal{R}_j; \tau_{out}(\mathcal{R}_i))$: Probability to exit region \mathcal{R}_i and enter region \mathcal{R}_j within the outflow time $\tau_{out}(\mathcal{R}_i)$

Comments

- For more details on "Landscape simplification" and "Useful static features", see [2, 3, 22, 23] and references cited therein.
- For more details on "Stability of locally ergodic regions", see [24]





Comments

- The threshold algorithm[25, 26] works as follows:
 - Find local minima
 - Choose a sequence of energy lids L_k . For a given lid L_k , perform long Monte Carlo walks where every move is accepted, unless it exceeds the energy of the lid. Every n_q moves, perform one or many quenches into the closest local minimum. Repeat the procedure with another lid.
 - From the energy lids where new minima are first found during one of the quenches, deduce an estimate for the barrier height between the starting minimum and the other minima.
 - From the distribution of energies encountered during the runs at various lids, deduce the local densities of states within the basin of the starting minimum.
 - Repeat the whole procedure for all other local minima observed.
 - Construct lumped tree for the energy landscape (yellow nodes indicate lumps; size of purple ellipses indicates the amount of states in a lump).
- Note that this method also works as an optimization procedure, i.e., one often finds new local minima not detected with the standard global minimization procedure. In some ways it behaves as a cousin of various "bouncing" or "cycling" algorithms.
- The transition probabilities determined by this algorithm between the local minima include both energetic, entropic and kinetic contributions.

Structure prediction: general procedure

- Locally ergodic regions on time scale t_{obs}
- Local free energy
$$F(\mathcal{R}) = -k_B T \ln Z(\mathcal{R})$$
- Probability (for $t_{obs} \rightarrow \infty$) to find region \mathcal{R} :
$$p(\mathcal{R}) = \sum_{i \in \mathcal{R}} p(i) = \frac{1}{Z_{ges}} \sum_{i \in \mathcal{R}} \exp(E_i/k_B T) = \frac{Z(\mathcal{R})}{Z_{ges}} = \frac{1}{Z_{ges}} \exp(-F(\mathcal{R})/k_B T)$$
- $\text{Max}_{\mathcal{R}} p(\mathcal{R}) \Leftrightarrow \text{Min}_{\mathcal{R}} F(\mathcal{R})$
- Consistency check: $p_{rest} = 1 - \sum_{\mathcal{R}} p(\mathcal{R})$
- Crystalline systems: p_{rest} small
- Amorphous systems: p_{rest} large?
Non/Quasi-equilibrium situation \Rightarrow Investigation of dynamics and completely accessible model systems, respectively, necessary

Comments

- The general procedure applies for all temperatures and all kind of chemical and physical systems. It is truly "general".
- If we are on time scales, where many locally ergodic regions are in local equilibrium, the one we are most likely to observe at a given experiment is the one with the lowest free energy. Thus, we would need to perform a minimization of the local free energy over all locally ergodic regions. Note that the space of locally ergodic regions consists of exceedingly many but isolated "points", i.e., mathematically we do not have the local free energy as a continuous function of \mathcal{R} .
- Sometimes, people write down an continuous order parameter \vec{M} , which allows us to parametrize the full configuration space, and then they calculate the free energy as function of the order parameter. Note that the region of the landscape that corresponds to a given value of this order parameter \vec{M} is usually not locally ergodic, however. At best, we can divide the coordinates into those degrees of freedom that equilibrate very quickly among themselves, and the remaining ones that vary more slowly (typically called reaction coordinates). If the number of fast degrees of freedom that are decoupled vastly exceeds the number of reaction coordinates, we can approximate the full free energy on short time scales by reduced free energies - computed only with respect to the fast degrees of freedom - that are parametrized by the reaction coordinates (essentially a separation of time scales approach).

Structure prediction through global exploration of energy landscapes of chemical systems

- General approach

- Determine structure candidates = locally ergodic regions
($T \approx 0$: \mathcal{R} centered on local minima \vec{R}_{min})
- Analyze the stability of the candidates
($T \approx 0$: Energy barriers E_B control $\tau_{esc} \propto \exp(E_B/kT)$)
- Calculate local free energies
($T \approx 0$: Phonon free energy $F_{vib} = kT \sum_{\vec{q}} \ln(\sinh(h\nu_{\vec{q}}/2kT))$)

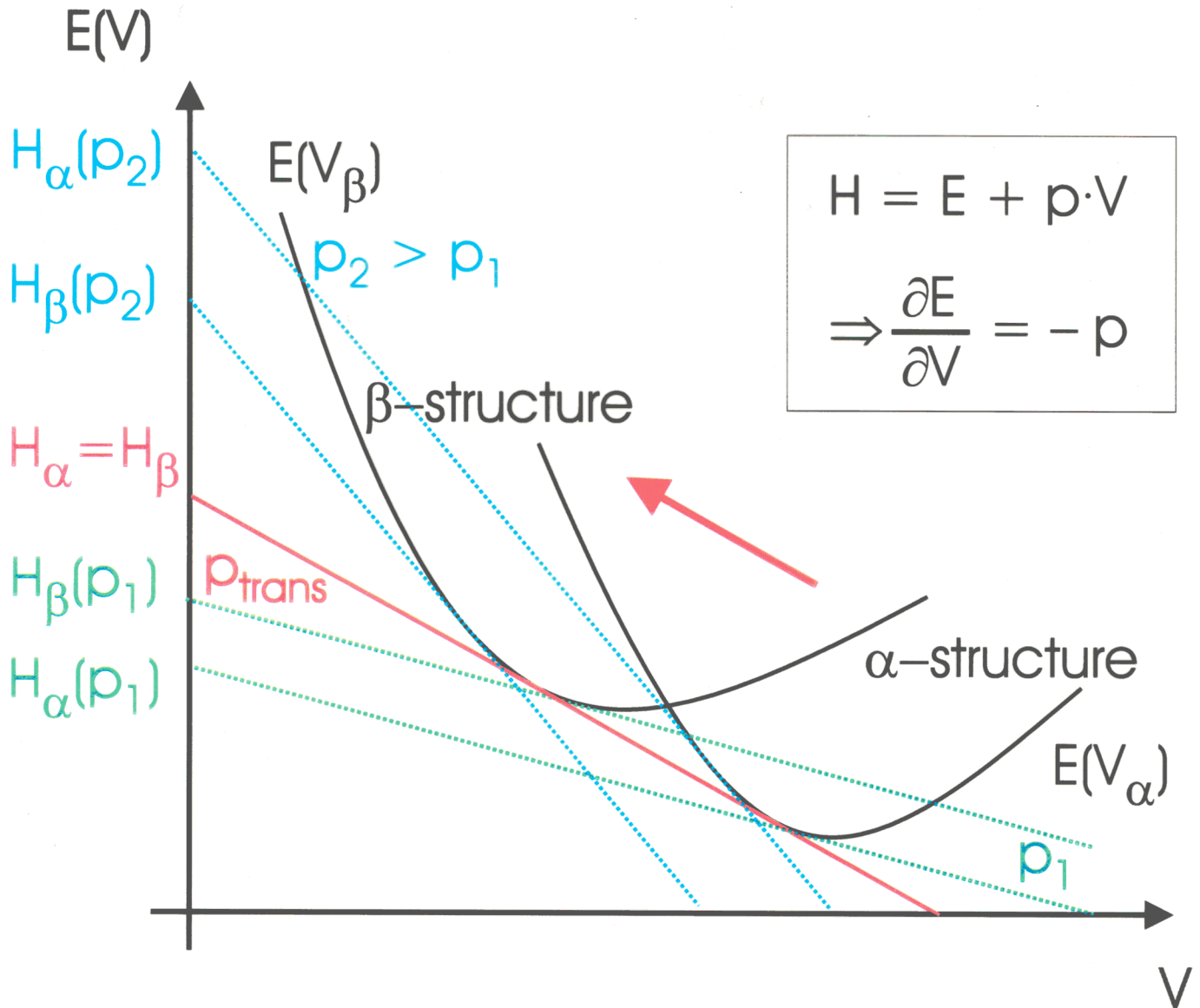
- Implementation

- Global optimization with simulated annealing
(atom / building unit / cell parameter variation, charge transfer, etc.)
on the empirical potential energy / enthalpy landscape
($p = 0, p \neq 0$) with periodic boundary conditions
- $E = \sum_{\langle IJ \rangle} V(r_{IJ}) + \sum_I E_{ion}(q_I) + pV$
$$V(r_{IJ}) = \frac{q_I q_J}{4\pi\epsilon_0 r_{IJ}} + \epsilon_{IJ} \left[\left(\frac{\sigma_{IJ}}{r_{IJ}} \right)^{12} - \left(\frac{\sigma_{IJ}}{r_{IJ}} \right)^6 \right]$$
- Stability analysis and local DOS
with the threshold algorithm
- Determination of symmetries of structure candidates
with SFND and RGS
- Local optimization of the structure candidates on ab initio
level using nested sequence of line searches
- (Determination of vibrational and electronic properties)

Comments

- In practice, we can only deal with the case $T \approx 0$ K (given in brackets).
- At low temperatures, escape times are controlled by energy barriers.
- At low temperatures, the most important contribution to the local free energy of insulators is due to the phonons.
- The actual implementation consists of several steps, since we cannot perform the global landscape exploration on ab initio level due to computational limitations: Global optimization with simple potential for a global exploration, followed by a local optimization with ab initio methods. In-between, several analysis, sorting and idealization steps need to be performed.

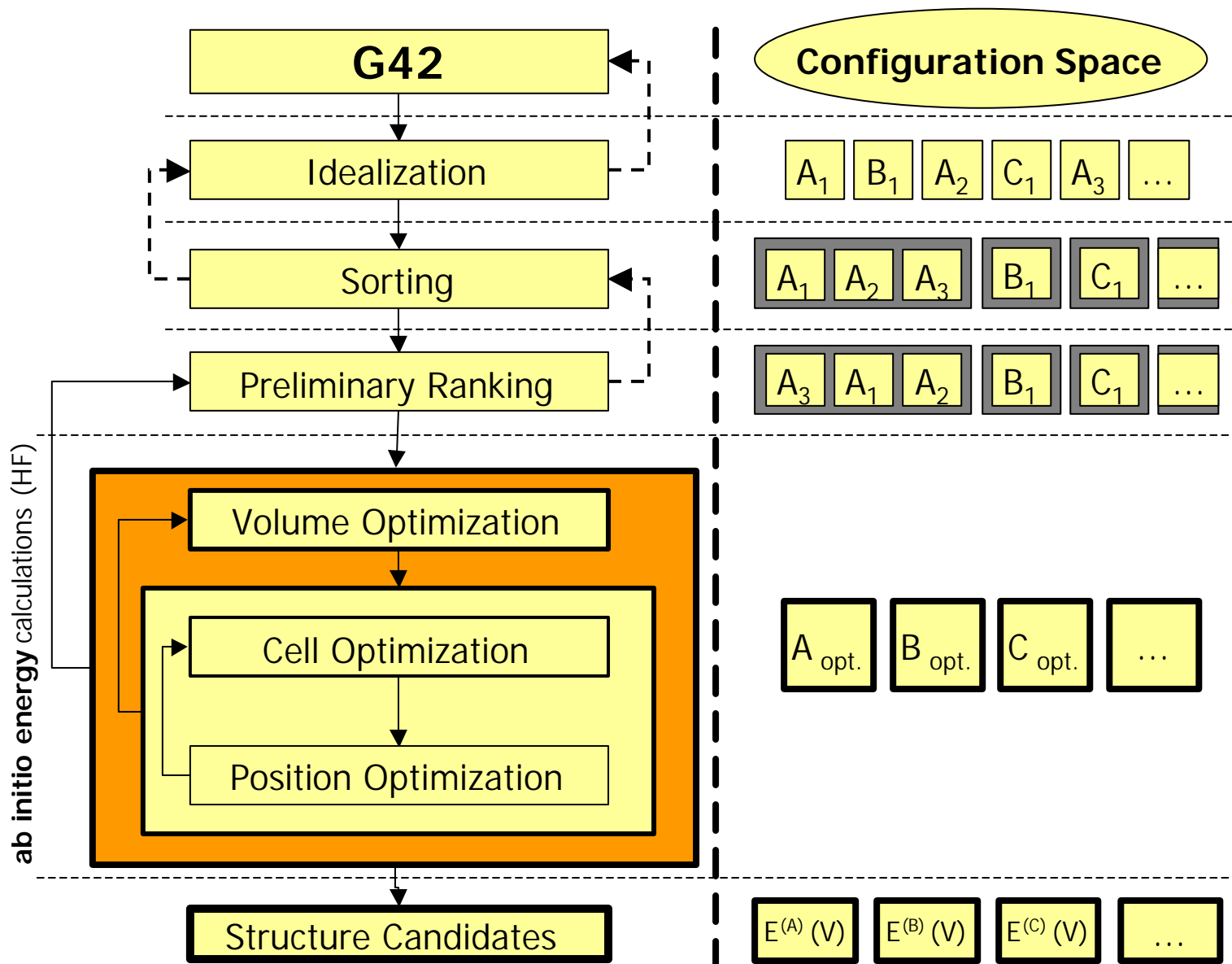
High pressure phase transition $\alpha \rightarrow \beta$



Comments

- From basic thermodynamics follows that the enthalpy of a modification i with energy curve $E_i(V)$ at a given pressure p is given by the y-axis intercept of the tangent to $E_i(V)$ with slope $-p$. The phase transition takes place when the enthalpies of two modifications are equal, i.e., the transition pressure is the negative slope of the common tangent between the two $E(V)$ curves.

Local optimization - Heuristic algorithm



Comments

- The ab initio level local optimization is implemented as a sequence of nested line searches[27].

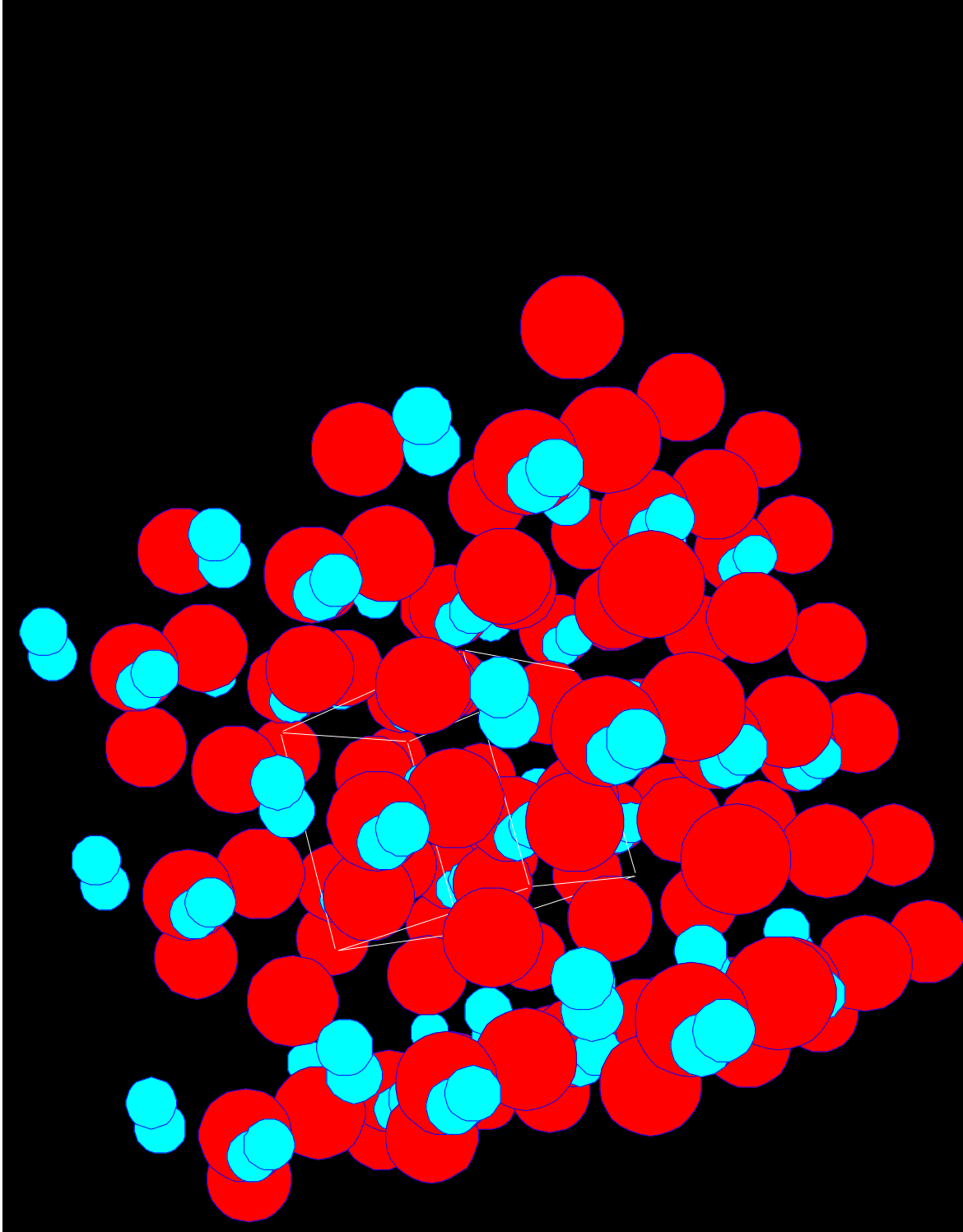


Figure 4: Initial configuration for NaCl-system.

Comments

- As a first example, we show some figures from the NaCl-system on the next few view graphs[17].
- The first one shows a typical random initial configuration in a periodically repeated simulation cell. The red spheres correspond to neutral Na-atoms, and the blue ones to neutral Cl-atoms, respectively. Their relative sizes correspond to their atomic radii.

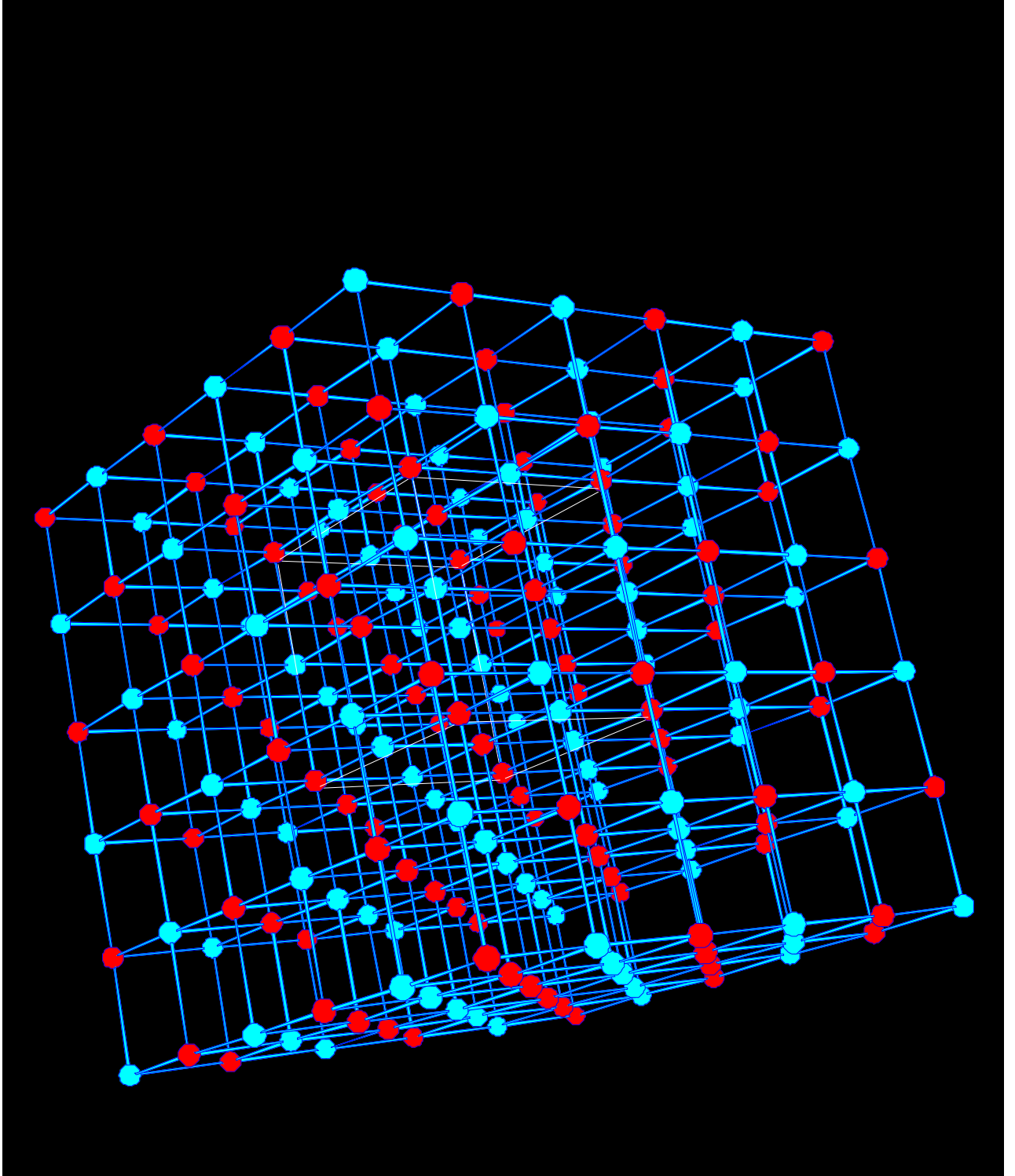


Figure 5: Structure candidate with rock salt structure for NaCl-system.

Comments

- One of the final structure candidates for the NaCl-system exhibiting the (experimentally observed) rock salt structure.
- Red and blue spheres now depict Na^+ - and Cl^- -ions, respectively. In order to exhibit the structure of the configuration, the radii of the spheres are set to 0.3 Ångstrom.

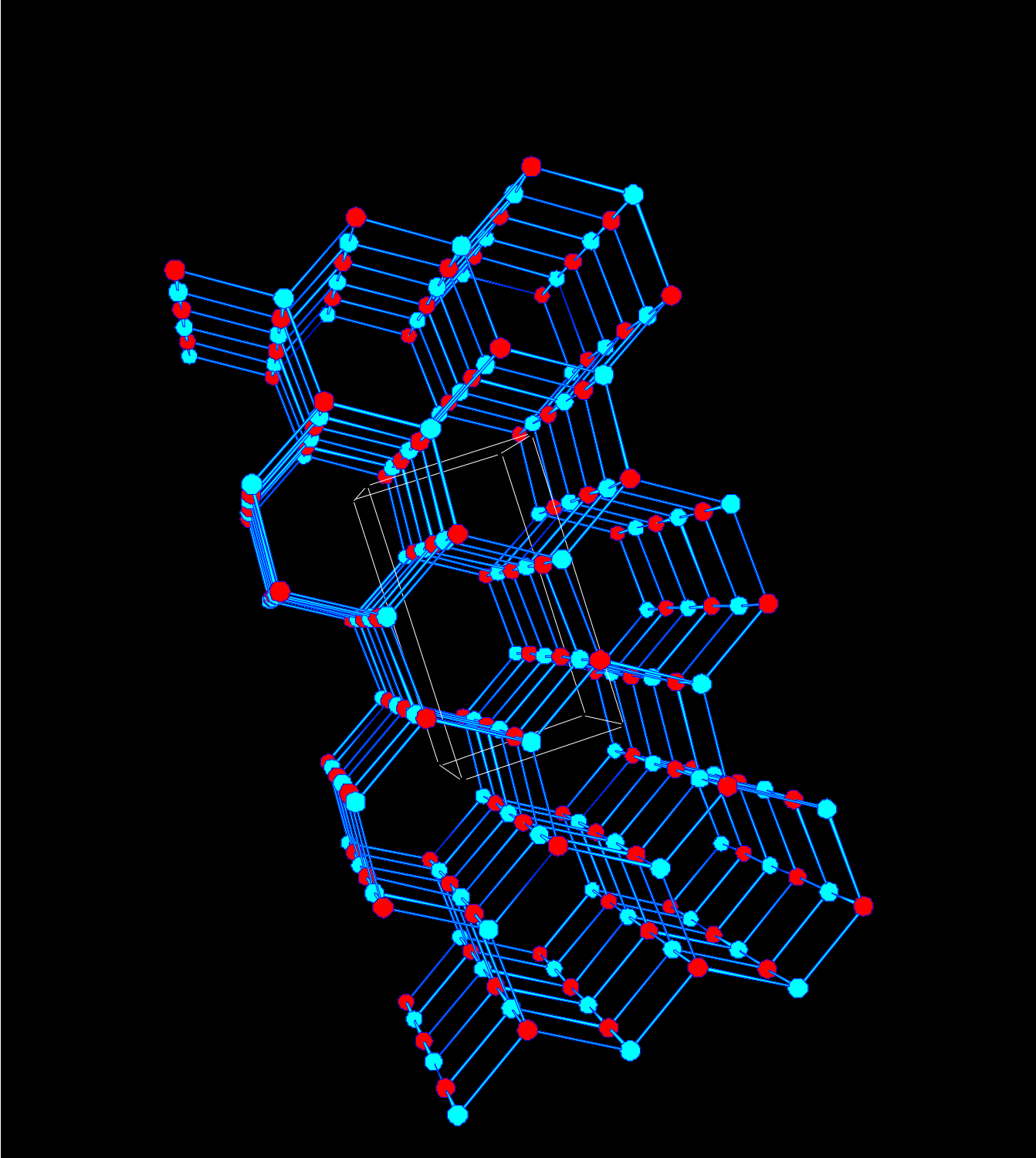


Figure 6: Structure candidate with 5-5 structure for NaCl-system.

Comments

- So-called 5-5 structure candidate for NaCl. The structure is an ionic variant of the h-BN-structure type.

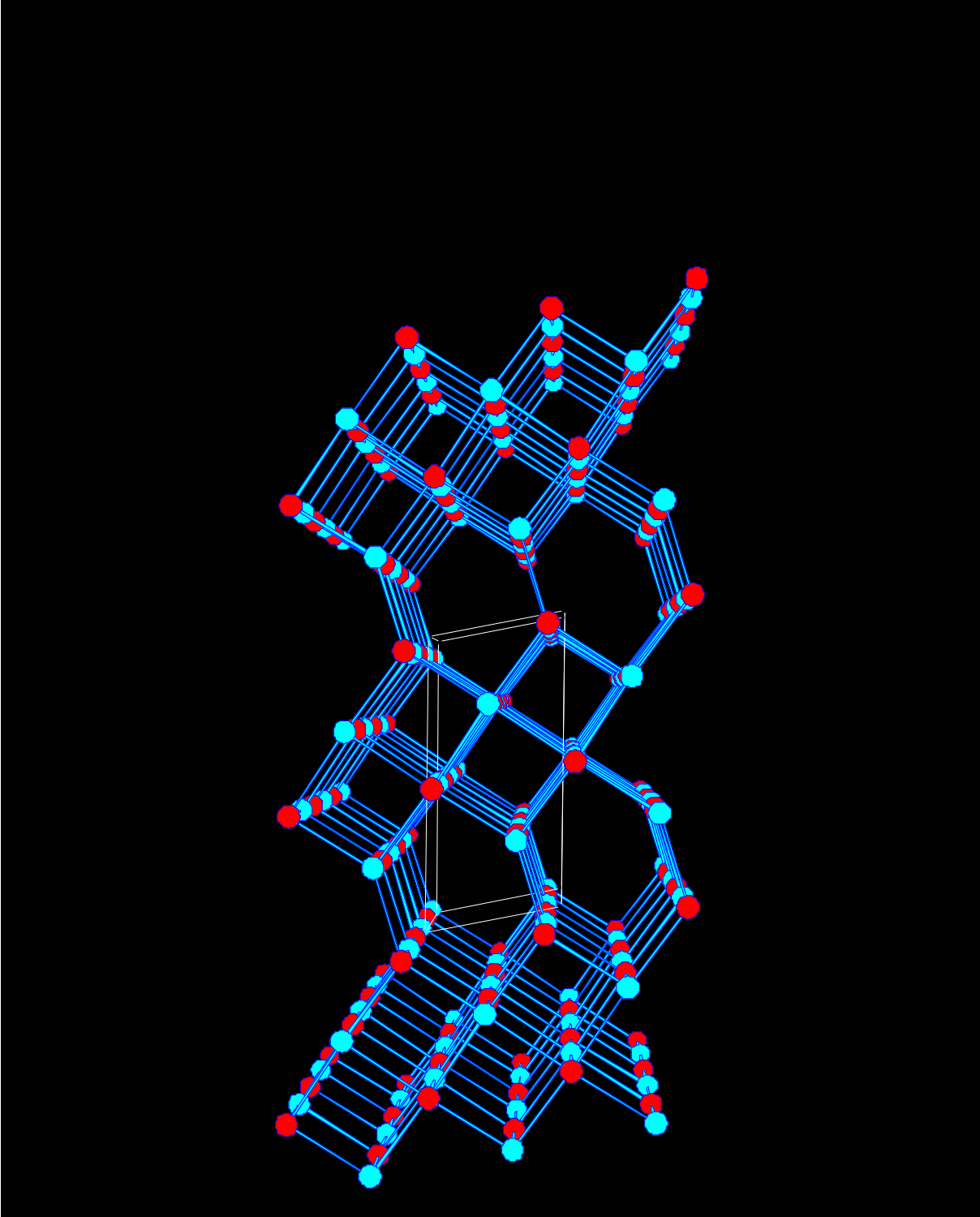
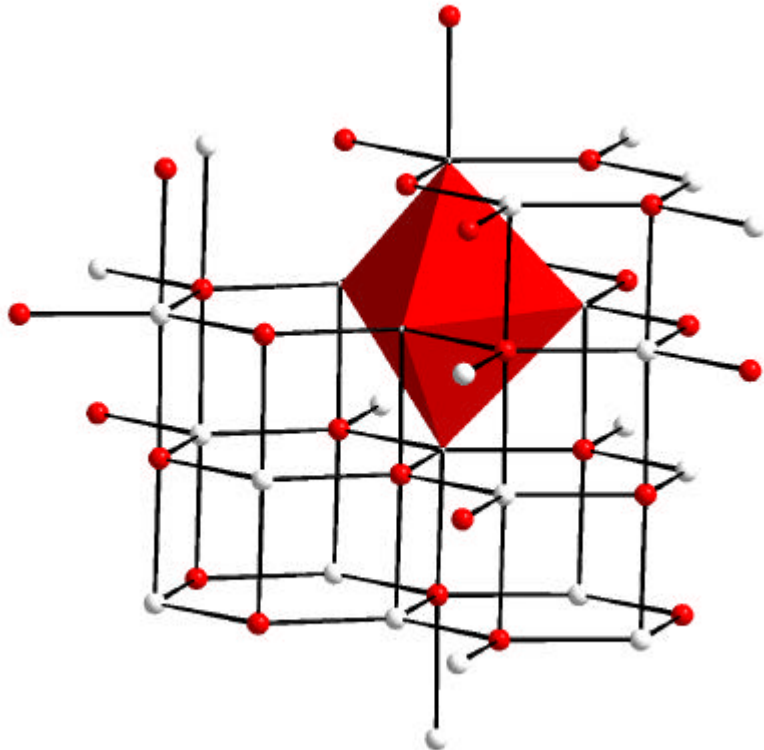


Figure 7: Structure candidate intermediate between rock salt and 5-5 structure for NaCl-system.

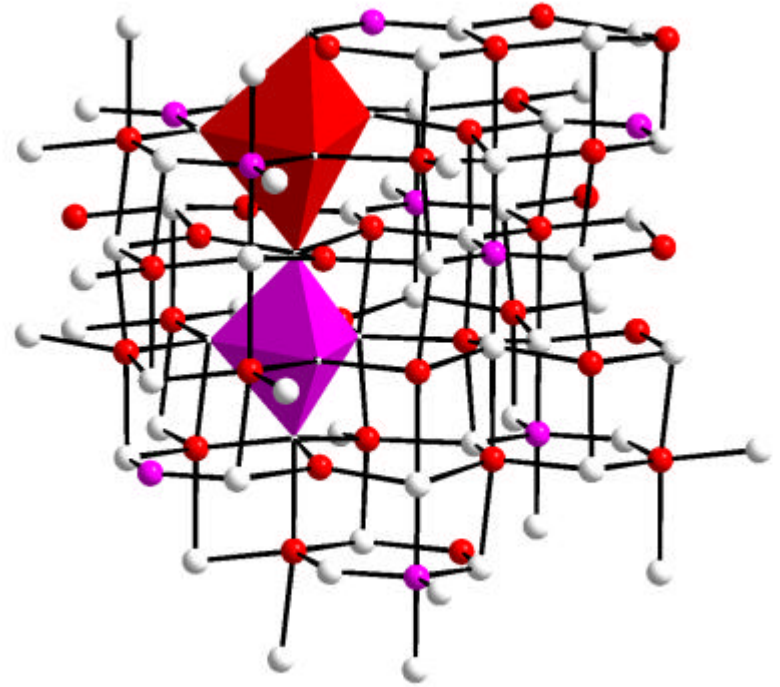
Comments

- Local minimum corresponding to an intermediate (transitional) structure between rock salt and 5-5 structure.
- With increasing number of atoms in the simulation cell, one tends to find more and more such intermediary structures. This can to a certain extent "clog" the global exploration procedure.

$A^{[5]}B^{[5]}$, a Predicted New Type of Structure



$\text{Na}^{[5]}\text{Cl}^{[5]}$



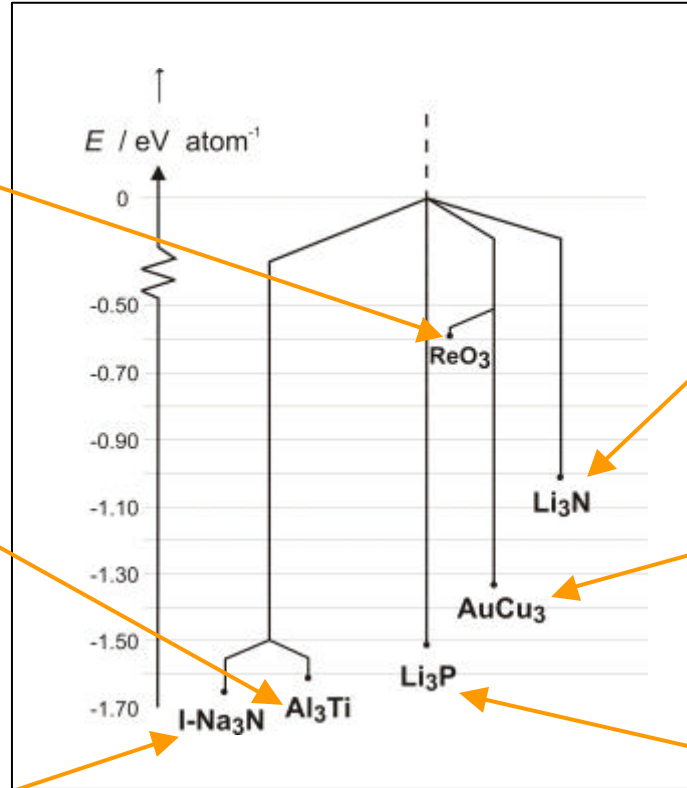
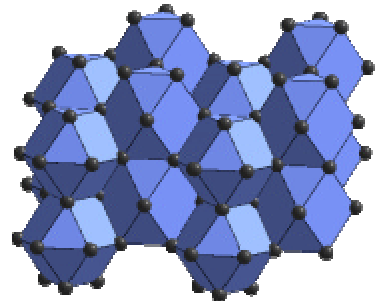
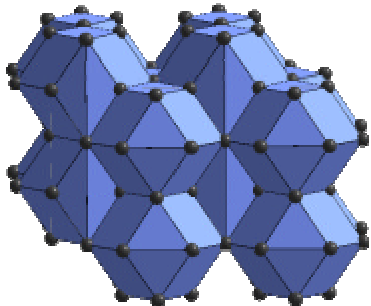
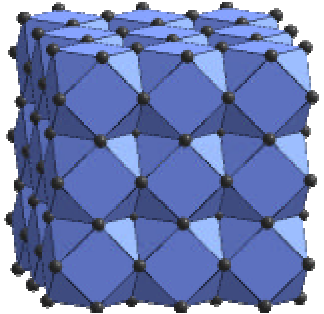
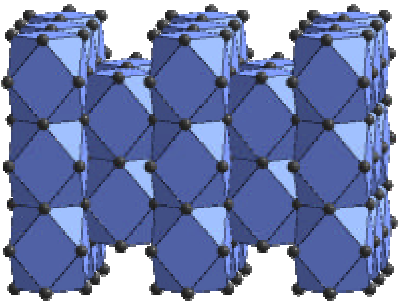
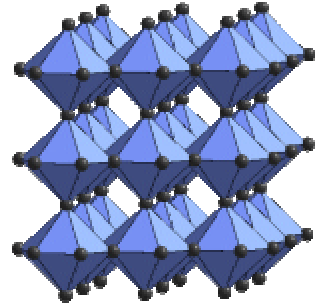
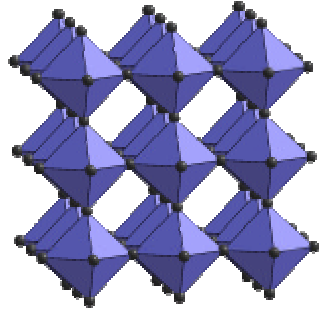
Li_4SeO_5

H. Haas and M. Jansen, *Angew. Chem.*, 1999

Comments

- The 5-5 type is a new ionic structure type that had not been observed until found during the global optimizations. However, recently, this structure type was found to be the aristotype of the ternary ionic compound Li_4SeO_4 [28].

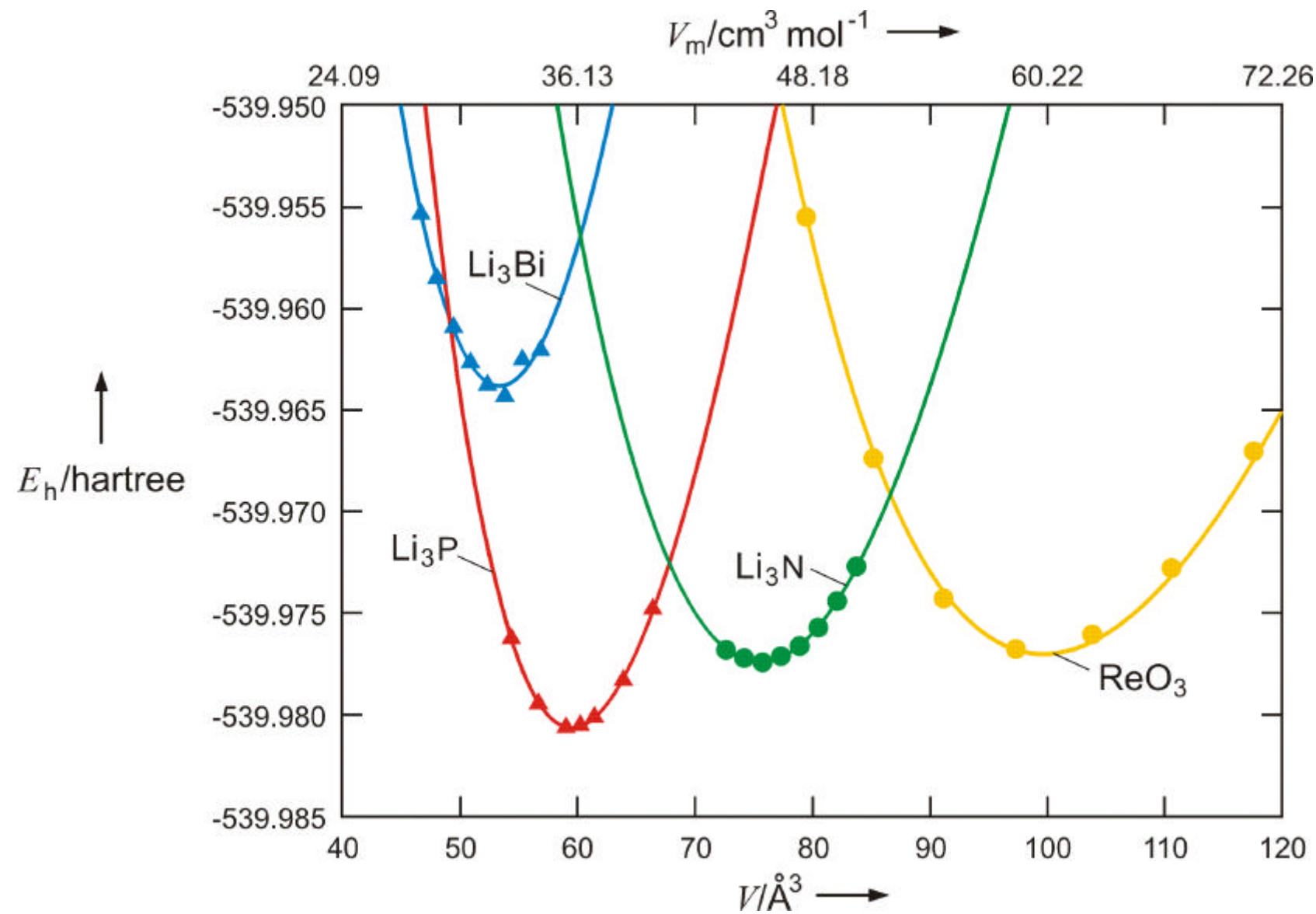
Energy landscape and structures of Na_3N



Comments

- Example: Na_3N -system
- Treegraph with some of the many local minima observed in this system[29]. Note that the energies are computed with the simple empirical potential.

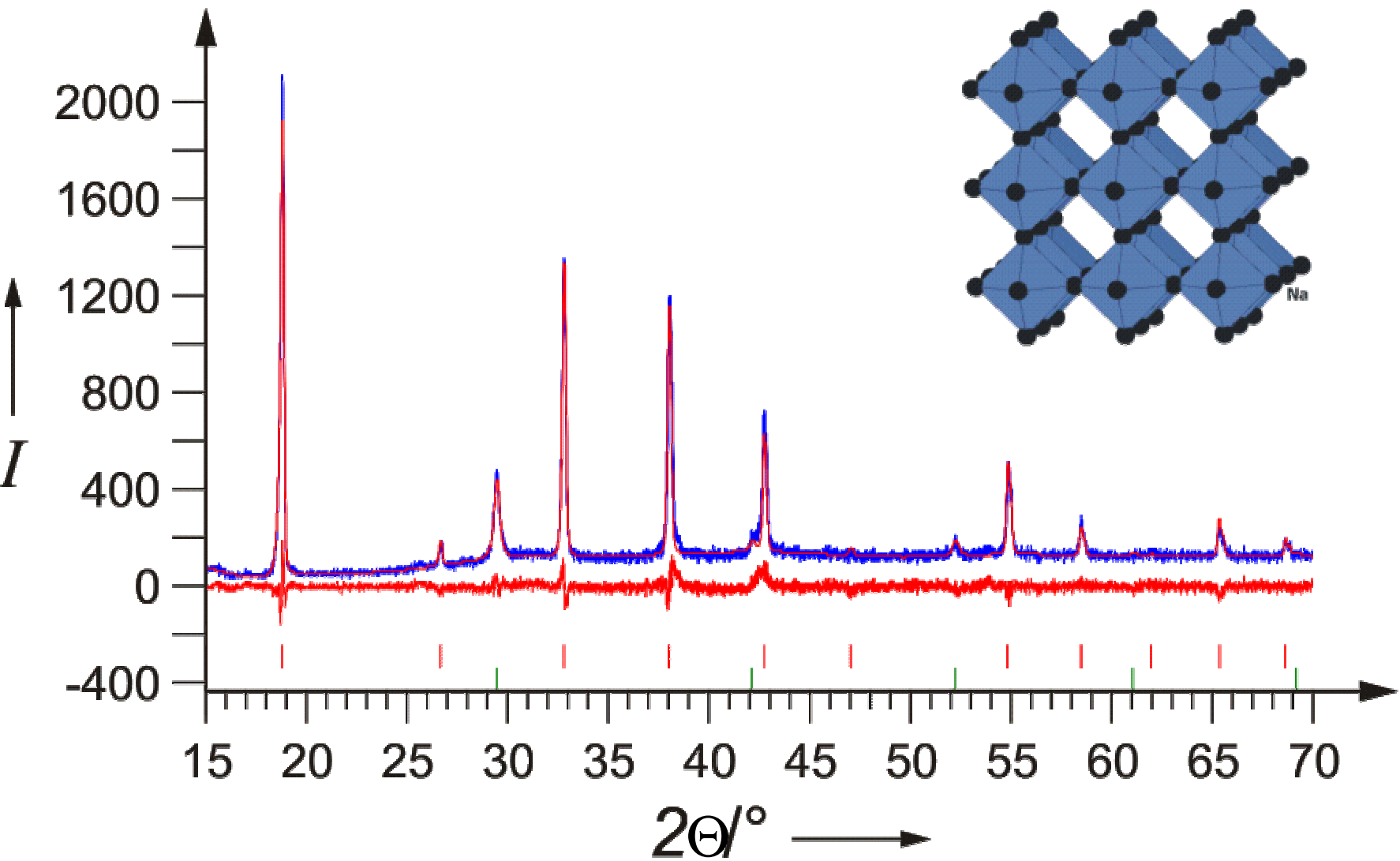
E(V) curves for promising structure candidates in the system Na₃N



Comments

- $E(V)$ curves found with ab initio energy calculations for selected candidates in the N_3N -system.
- Note that for this only moderately ionic system the candidates with the lowest ab initio energies are not identical with the ones for the empirical potential. This contrasts with e.g. the NaCl or the MgF_2 system, where ab initio and empirical potential yield the same sequence of candidates by energy.

Powder diffraction pattern for Na₃N (Rietveld refinement) and structure candidate (anti-ReO₃ type)



Comments

- Experimental results for the Na_3N -system using low temperature atom deposition methods for the synthesis[30]
- Interestingly enough, the structure synthesized by the atom deposition method is the one with the lowest density, not the one with the lowest energy. This is connected to the specific aspects of the procedure: First, atoms are deposited randomly on a very cold substrate, where an amorphous solid is formed. Upon heating, crystallization begins locally within the amorphous matrix. Since the crystalline nuclei are more dense than the surrounding matrix, they experience an effective negative pressure from their environment. This negative pressure favors the formation of the low-density phase.

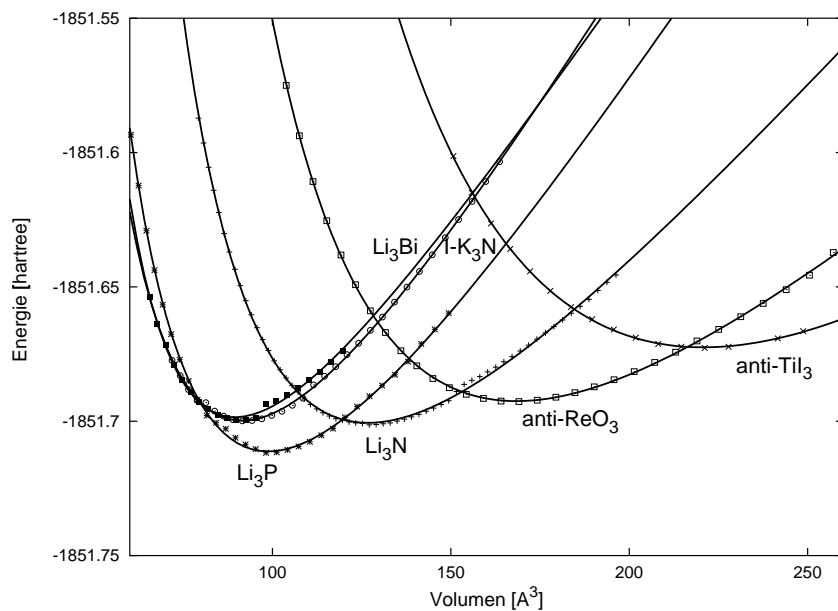


Figure 10: $E(V)$ -curves on HF-level for structure candidates in K_3N -system.

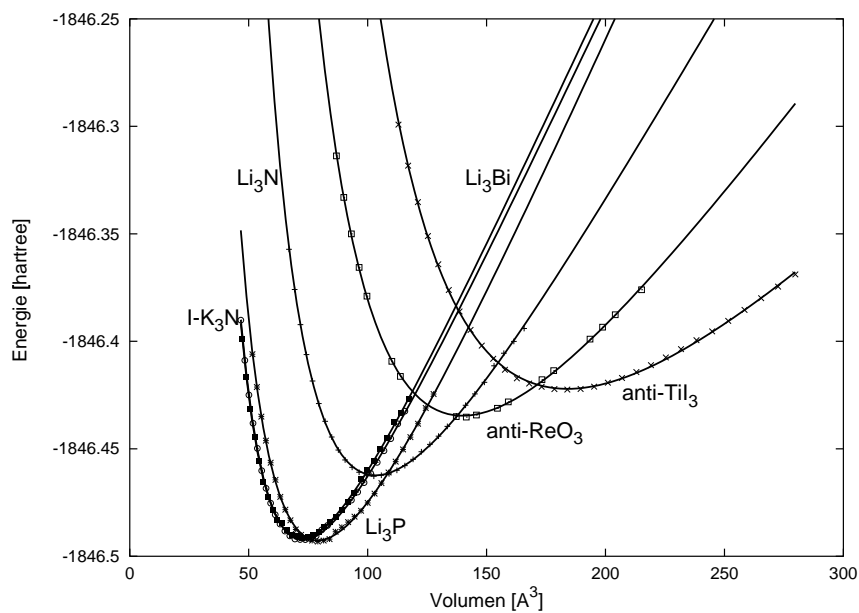


Figure 11: $E(V)$ -curves on DFT-level for structure candidates in K_3N -system.

Comments

- Example K_3N [31]
- Two sets of $E(V)$ -curves generated with different ab initio methods (Hartree-Fock and DFT-LDA-VBH). From over thirty structure candidates, only the six with lowest energy are shown.

K/N Codeposition

substrate:

sapphire ((0001), epitaxial polished)

temperature:

77 K

K:

effusion cell (373 K)

N₂:

MW-plasma source (1.6 sccm, 80 mA, purity 5.0)

process pressure:

6×10^{-5} mbar

time:

5 h

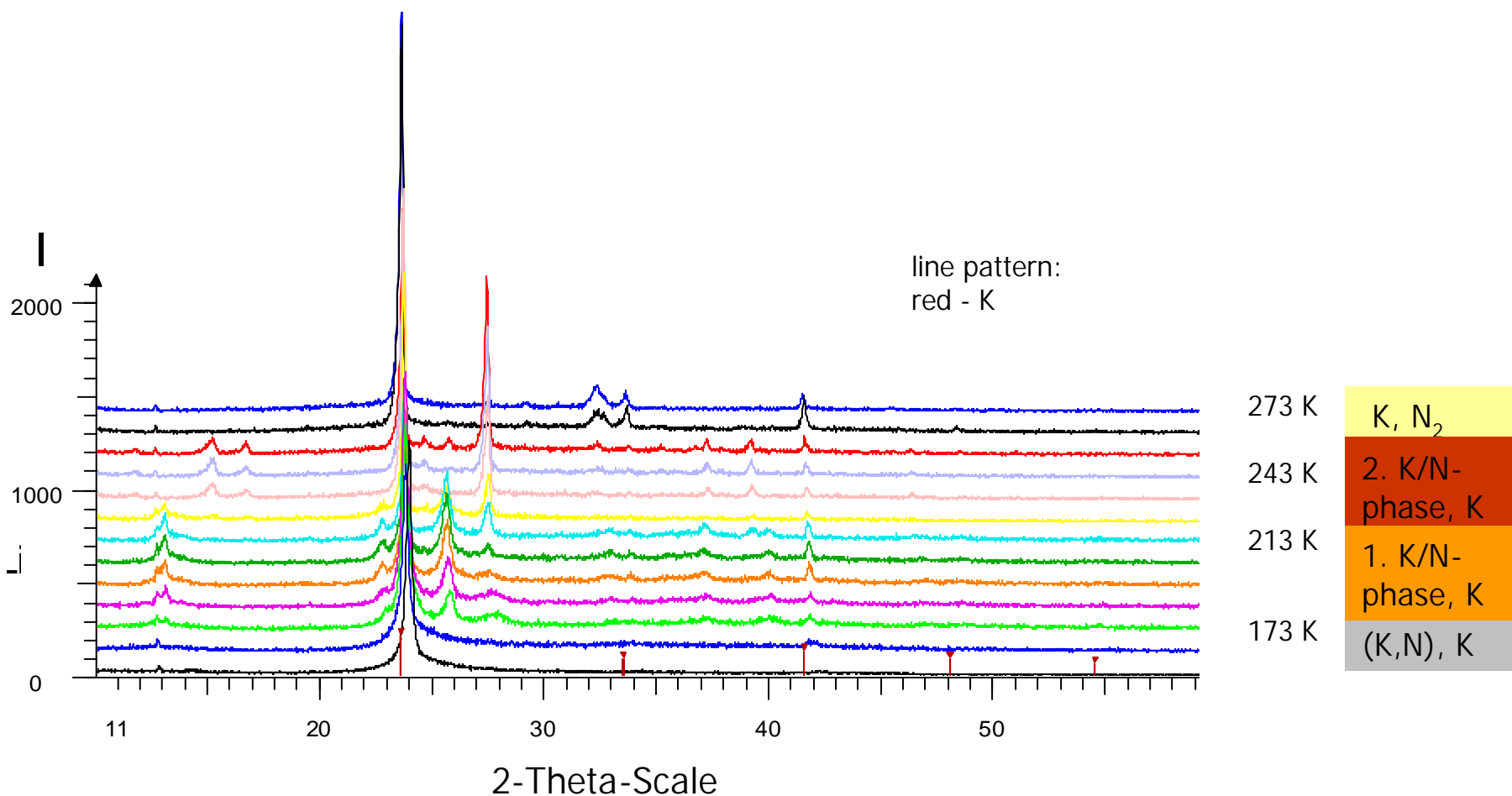
sample:

metallic color

XRD:

temperature-dependent, potassium nitride?

Temperature-dependent X-ray powder diffraction of K/N

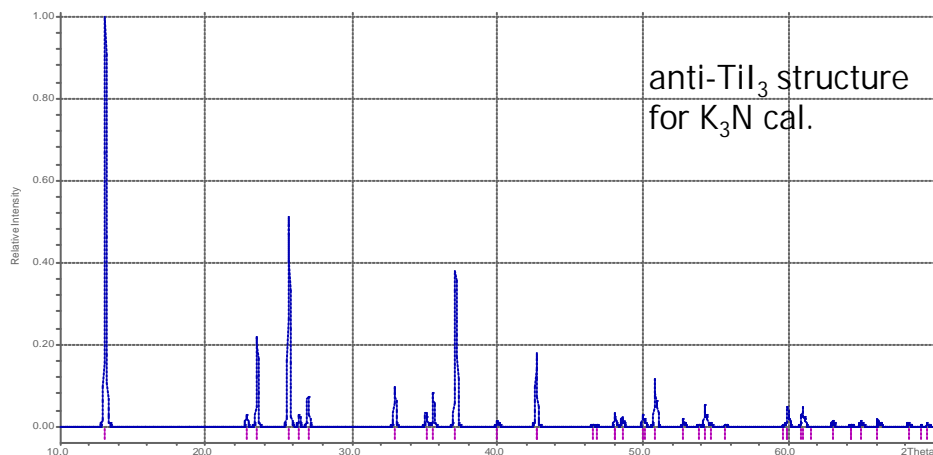
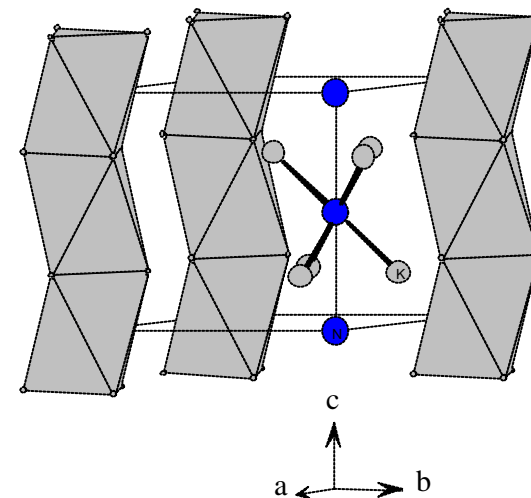
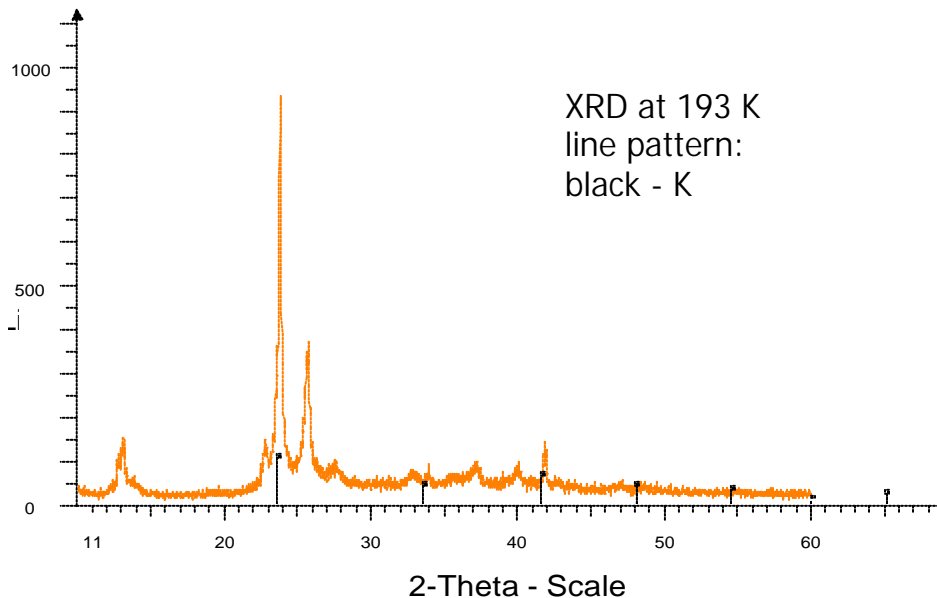


single scans: 77, 153, 173, 183, 193, 203, 213, 223, 233, 243, 253, 263, 273 K; line diagram: K

Comments

- Powder diffractogram as function of temperature taken during the heating phase starting at liquid nitrogen temperature.

X-ray powder diffraction pattern: 1. K/N phase

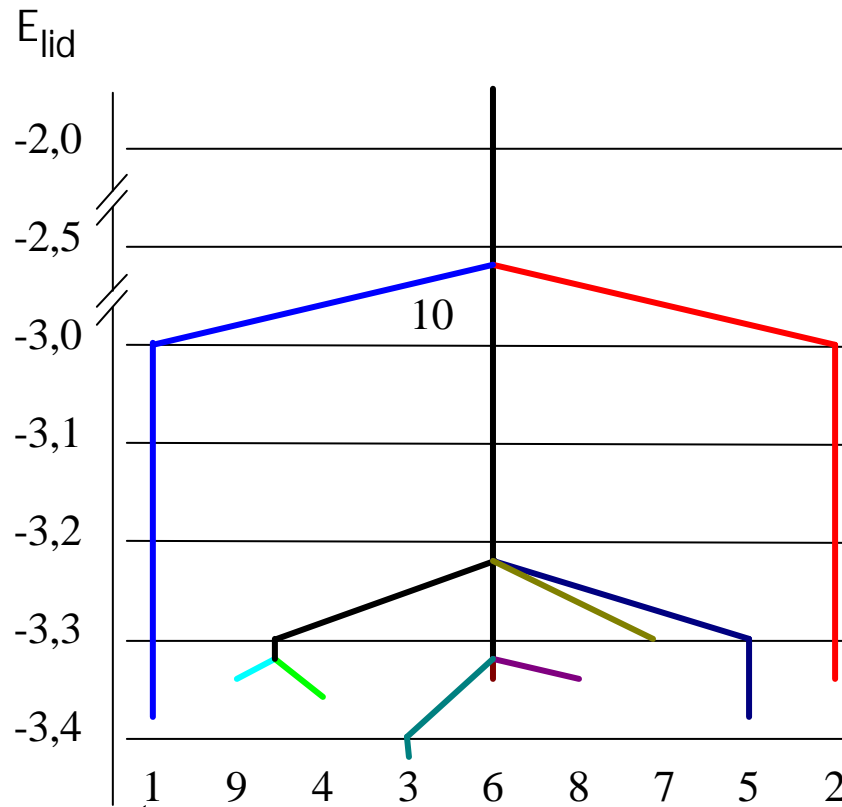


K₃N: anti-TiI₃ structure type
hex., $P 6_3/mcm$ (No. 193)
 $a=780$, $c=759$ pm, $\beta=120^\circ$
 $Z=2$, $V=120$ cm³/mol,
K: (6g), N: (2b)
 $d(K-N)=278$ pm

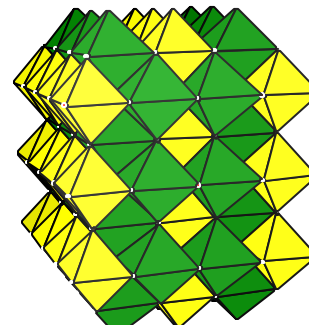
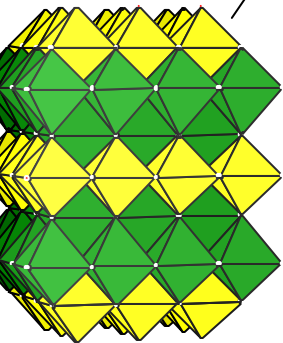
Comments

- The first structure candidate found appears to exhibit a TiI_3 -type structure.
- Again, this structure corresponds to the candidate that would be thermodynamically stable at negative pressures.

Energy landscape and structures of Ca_3SiBr_2



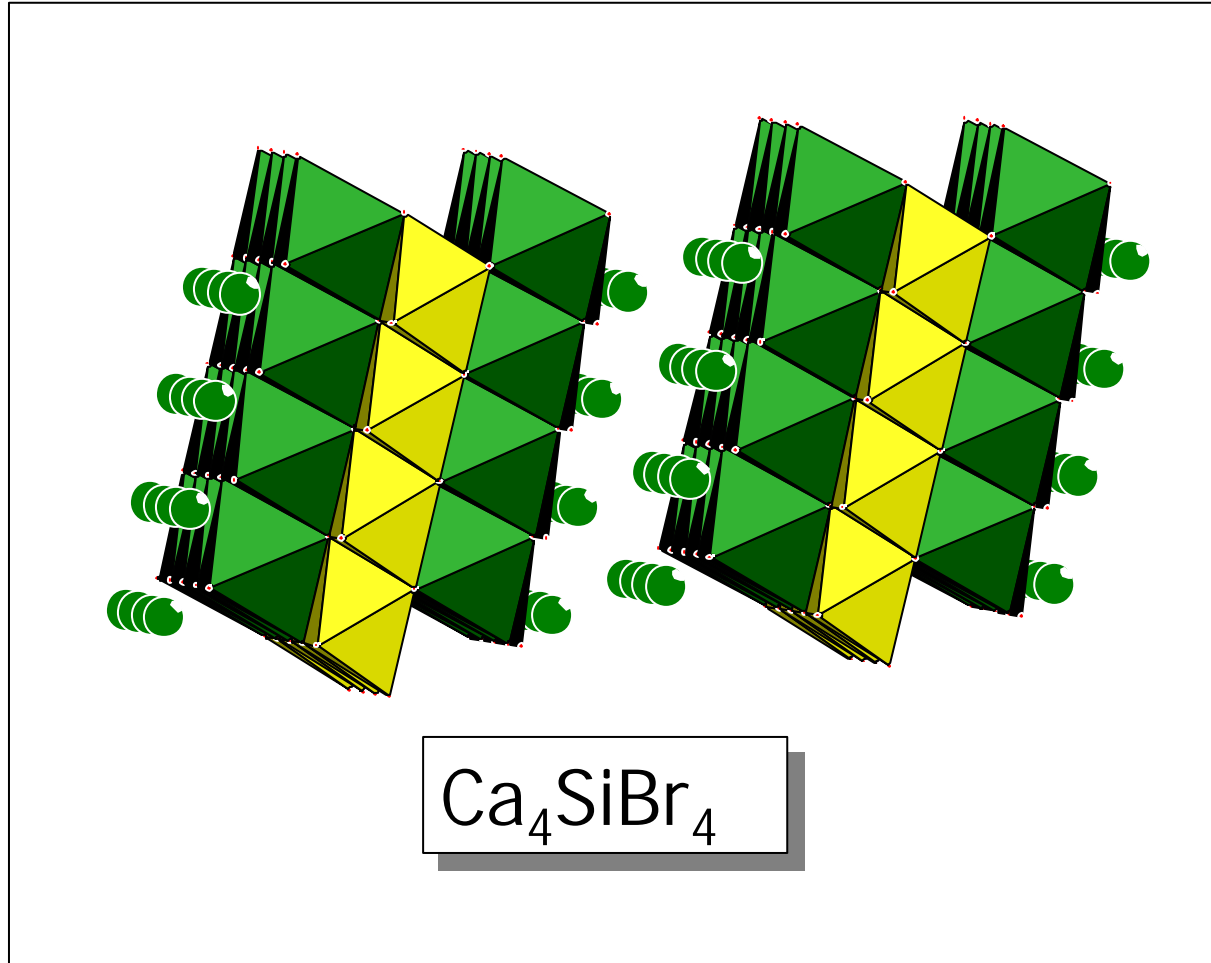
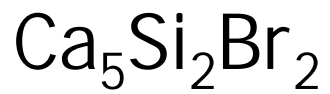
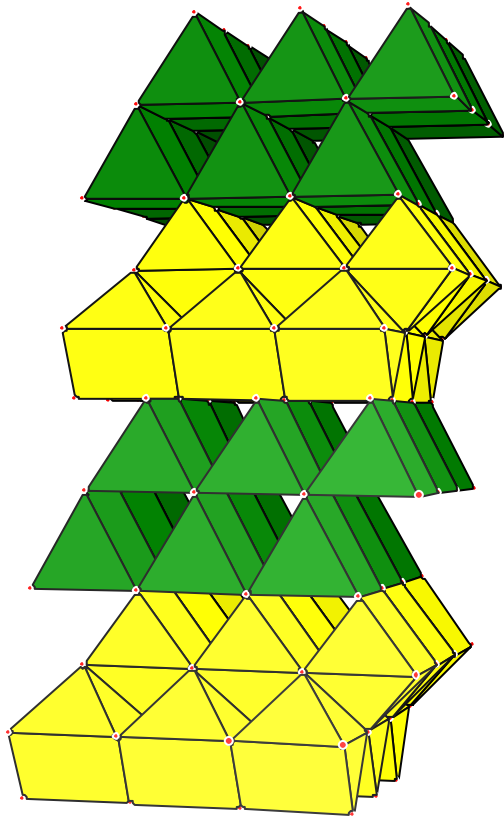
Strukture	E_{HF} [eV/Atom]
1	-34,3547
2	-34,3492
3	-34,0825
4	-34,0308
5	-33,9138
6	-34,0526
7	-33,9301
8	-34,1342
9	-34,1206
<hr/>	
CaBr_2	-31,5110
Ca_2Si	-36,9261
Mean Value	-34,2186



Comments

- Example: Ca/Si/Br-system[32]
- Tree graph for the composition Ca_3SiBr_2
- Two especially favorable structure candidates, both exhibiting the NaCl-aristotype.
- In a related system (Ba_3SiI_2), also a NaCl-superstructure has been observed.
- Comparison of ab initio energies of the structure candidates for Ca_3SiBr_2 and the weighted sum of the binary systems Ca_2Si and CaBr_2 .
- The ternary compound appears to be more thermodynamically stable than the mixture of the binary compounds.

Variation of the composition



Comments

- Structure candidates for different compositions in the Ca/Si/B-system.
- The ab initio calculations for the alternative compositions show that the optimal combination appears to be Ca_3SiBr_2 .

RUN	Transition	System																	
		Li ₂ S			Na ₂ S			K ₂ S			Rb ₂ S			Cs ₂ S					
		Calc. [GPa]	Obs. [GPa]		Calc. [GPa]	Obs. [GPa]		Calc. [GPa]	Obs. [GPa]		Calc. [GPa]	Obs. [GPa]		Calc. [GPa]	Obs. [GPa]				
HF	anti-CaF ₂ → PbCl ₂	26.8	8-20	6.4 ^t	7	2.7	-	1.9 ^t	-	1.9 ^t	-	1.3 ^t	-	1.7 ⁱⁱ	-	1.3 ^t	-		
	PbCl ₂ → anti-Ni ₂ In	-	-	24.7 ^t	16	6.5	-	4.5 ^t	-	7.1 ⁱⁱ	-	6.9 ^t	-	64.70 ⁱⁱⁱ	-	6.9 ^t	-		
	PbCl ₂ → anti-Ni ₂ In-dist.	-	-	15.6 ^t	-	6.4	-	-	-	0.39 ⁱⁱⁱ	-	-	-	7.7 ⁱⁱⁱ	-	-	-		
	anti-CaF ₂ → anti-Ni ₂ In	-	-	-	-	4.1	6	1.02 ⁱⁱⁱ	-	-	-	-	-	9.2 ⁱⁱ	-	-	-		
DFT (LDA VBH)	anti-CaF ₂ → PbCl ₂	14.0	8-20	2.7 ^t	7	1.0	-	1.3 ^t	-	0.8 ⁱⁱ	-	2.9 ^t	-	0.26 ⁱⁱ	-	2.9 ^t	-		
	PbCl ₂ → anti-Ni ₂ In	28.8	-	12.4 ^t	16	1.9	-	2.8 ^t	-	3.2 ⁱⁱ	-	1.03 ^t	-	-	-	1.03 ^t	-		
	PbCl ₂ → anti-Ni ₂ In-dist.	40.6	-	12.5 ^t	-	2.0	-	11.4 ⁱⁱ	-	2.7 ^t	-	1.33 ^t	-	7.0 ⁱⁱ	-	1.33 ^t	-		
	anti-CaF ₂ → anti-Ni ₂ In	-	-	11.6 ⁱⁱ	-	1.4	6	-	-	3.1 ⁱⁱ	-	2.1 ⁱⁱⁱ	-	2.1 ⁱⁱⁱ	-	2.15 ^t	-		
DFT (LDA LYP)	anti-CaF ₂ → PbCl ₂	12.7	8-20	1.9 ^t	7	0.15	-	0.9 ^t	-	0.37 ⁱⁱ	-	2.2 ^t	-	-0.35 ⁱⁱ	-	2.2 ^t	-		
	PbCl ₂ → anti-Ni ₂ In	29.4	-	10.8 ^t	16	-0.12	-	10.8 ^t	-	1.6 ^t	-	0.348 ^t	-	-1.4 ⁱⁱⁱ	-	0.348 ^t	-		
	PbCl ₂ → anti-Ni ₂ In-dist.	24.3	-	8.9 ^t	-	-0.08	-	29.2 ⁱⁱ	-	1.4 ^t	-	0.653 ^t	-	4.3 ⁱⁱ	-	0.653 ^t	-		
	anti-CaF ₂ → anti-Ni ₂ In	-	-	9.1 ⁱⁱ	-	0.035	6	-	-	1.9 ⁱⁱ	-	-0.2 ⁱⁱⁱ	-	-0.2 ⁱⁱⁱ	-	1.52 ^t	-		

Table 1: Transition pressures for alkali metal sulfides

Comments

- Prediction of alkali metal sulfide transitions at high pressures[23, 33]
- Good agreement of predicted pressures with subsequent experimental observations where available[34, 35].
- Note the dependence of the actual numerical value of the transition pressures on the ab initio method used. Nevertheless, the sequence of structures as function of pressure (including negative pressure values) tends to be invariant under a change of ab initio methods.
- If possible, a full local optimization should be performed including variation of all cell parameters and atom positions that are not fixed by symmetry requirements.

Incorporation of external information - Cost functions and constraints

- Building units
 - Primary building units
 - * Rigid groups of atoms
 - * Constraints on atom-atom distances and angles
 - Secondary building units
 - * Rigid network fragments (e.g. polyhedra)
 - * Cost function with pseudo-interactions among building units
 - * Local optimization (ab initio or optimized potentials)
- Powder diffraction data
 - Information: cell parameters and cell content
Constraints: unit cell and composition kept fixed
 - Information: full powder diffractogram
Cost function: Linear combination of potential energy and the difference between measured and computed powder diffractogram
- Special cost functions
 - Bond-valence terms
 - Purely repulsive interactions in fixed unit cell

Comments

- For primary building units, see [18, 19, 20].
- For secondary building units, see [21, 20]
- Note: For structure prediction with primary building units, one needs to investigate different charge distributions over the building unit (i.e., repeat the optimization runs with different distributions), since one usually does not know the "correct" charge distribution a priori.
- Special cost functions are usually only usable when the unit cell is already fixed.

Primary building Units

- Preferred local environments during global optimisation

$$\implies \sum_{\alpha} \sum_{i,j \in \alpha} V_{ij} = \text{const.}$$

$$E' = pV + \sum_{\alpha,\beta} V_{\alpha,\beta} ; V_{\alpha,\beta} = \sum_{i \in \alpha, j \in \beta} V_{ij}$$

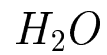
- "Known" building units from experiment

\implies Non-ionic aspects accessible

- Molecules
- "Free" electron pairs
- Complex ions
- Zintl ions
- ...

N_2

- Rigid molecule, with/without bond electrons
- Many structure candidates exhibiting chains and twisted N_2 -molecules
- Observed low temperature structure as candidate (space group $Pa\bar{3}$)
- Related/identical structure candidates for different charge distributions in N_2



- Rigid molecule, with formal charges (H^+ , O^{2-})
- Many candidates exhibiting network structures
- Christobalite-analogue as best candidate
(Ice Ic, $T_{exp} = 83K$)
- Similar networks for optimization with individual ions

SnO

- Structure not accessible with individual ions
(*Na – Cl*- instead of *Pb – O*-structure)

- "Free" electron pair bound to *Sn*,
with/without charge

- Structure candidates depend on orientation of electron pair
 - orthogonal to "plane":
 - * 2/4-coordination (square-planar / pyramid-like): "*Pb – O*"-structure
 - * 1/5-coordination
(layers with rocksalt-elements)
 - within "plane": 3/3-coordination (*Sn – Sn*-"bond"), e.g. rutile-like structures

KNO_2

- Experiment:
disordered $Na - Cl$ -super-structure at 300K

- $(NO_2)^{1-}$ strongly covalent,
different charge distributions

- Structure candidates dependent on charge of N
 - formal charges
→ layer-like structures
 - δ^+ at N
→ $Cs - Cl$ - and $Na - Cl$ -super-structure
 - δ^0, δ^- at N
→ $Na - Cl$ -super-structure

- Structure candidates $\hat{=}$ possible low-temperature structures

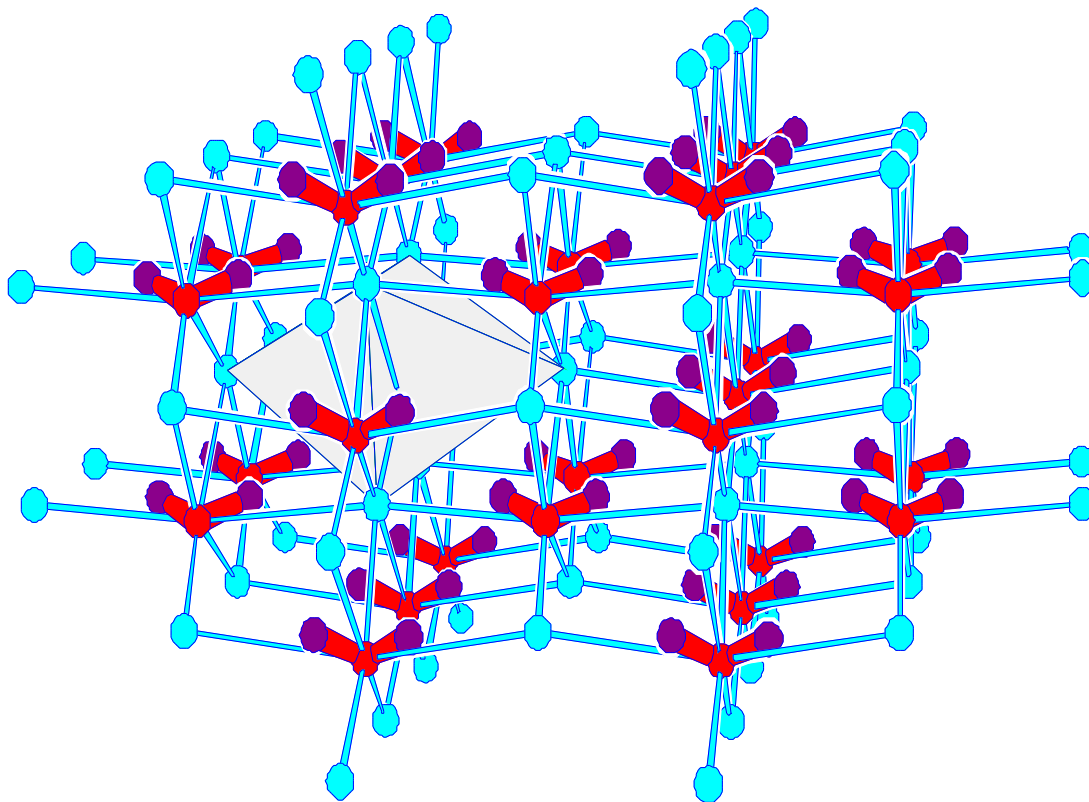


Figure 12:

One of the many structure candidates found during global optimizations of the KNO_2 -system, using NO_2 -building units, where the NK_6 -octahedra form a distorted rock salt structure, analogous to the observed high-temperature structure[36]. The space groups of these (possibly low-temperature) structure candidates ranged from e.g. $Cmca$ and $Pmna$ to $P1$, depending on the degree of order in the orientations of the NO_2 -units.

Comments

- Figure: Low-temperature structure candidate for KNO_2 . Note that the "high"-temperature structure known from experiment corresponds to a (rotationally) disordered structure, which shows the same NaCl-superstructure as the one found during the simulations, if one replaces K by Na and NO_2 by Cl.
- Many more low-temperature modifications are observed in the simulations, all corresponding to a different freezing-in of the orientation of the NO_2 -units.

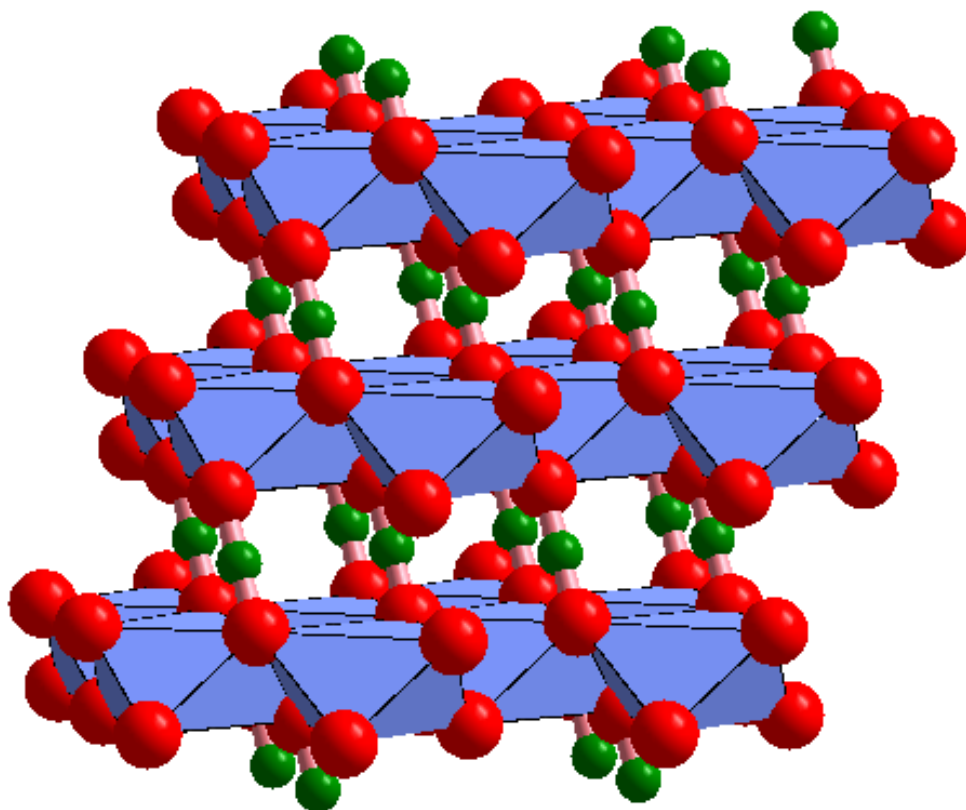


Figure 13:
Structure candidate corresponding to the experimentally observed structure for MgCN₂.

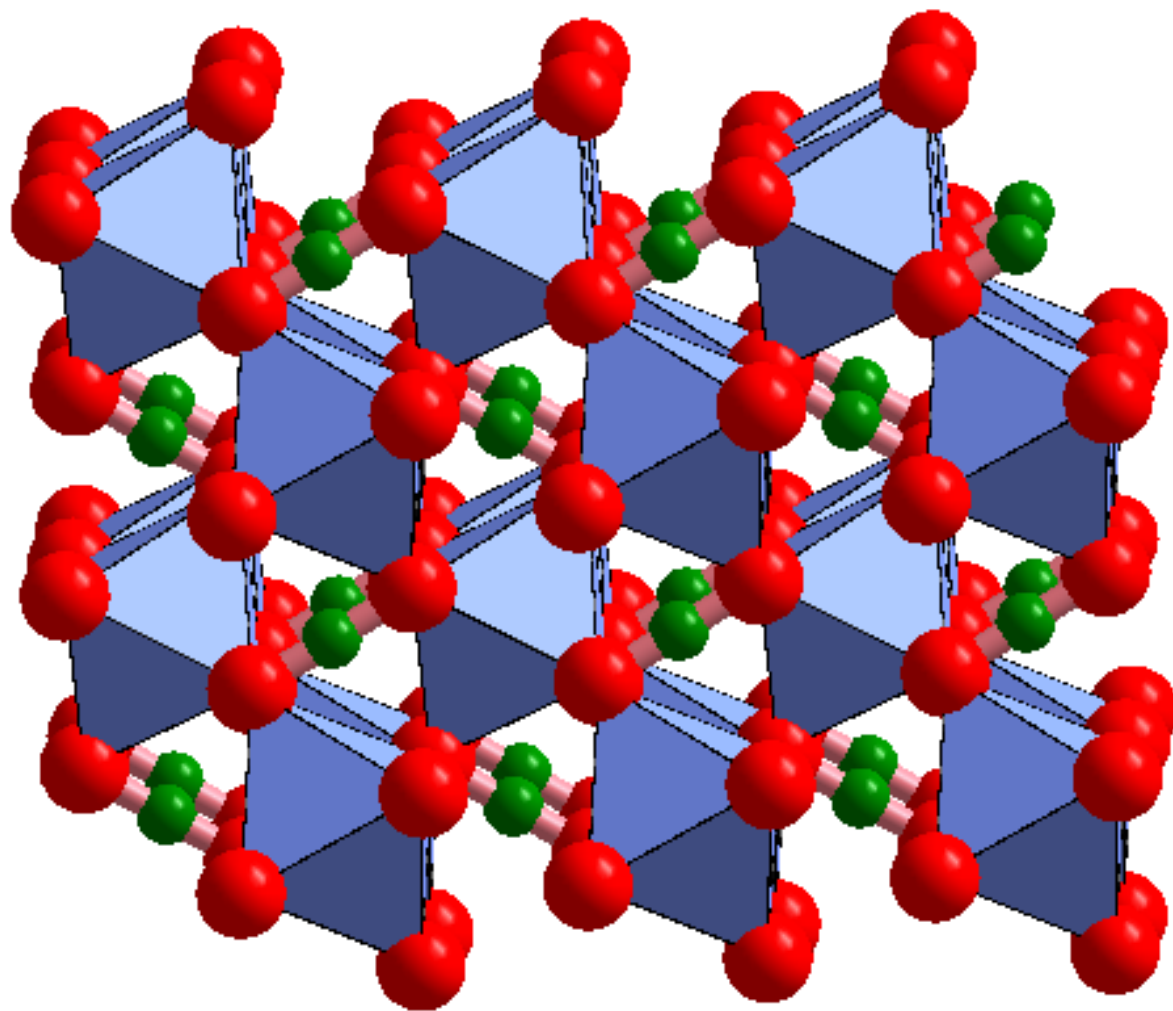
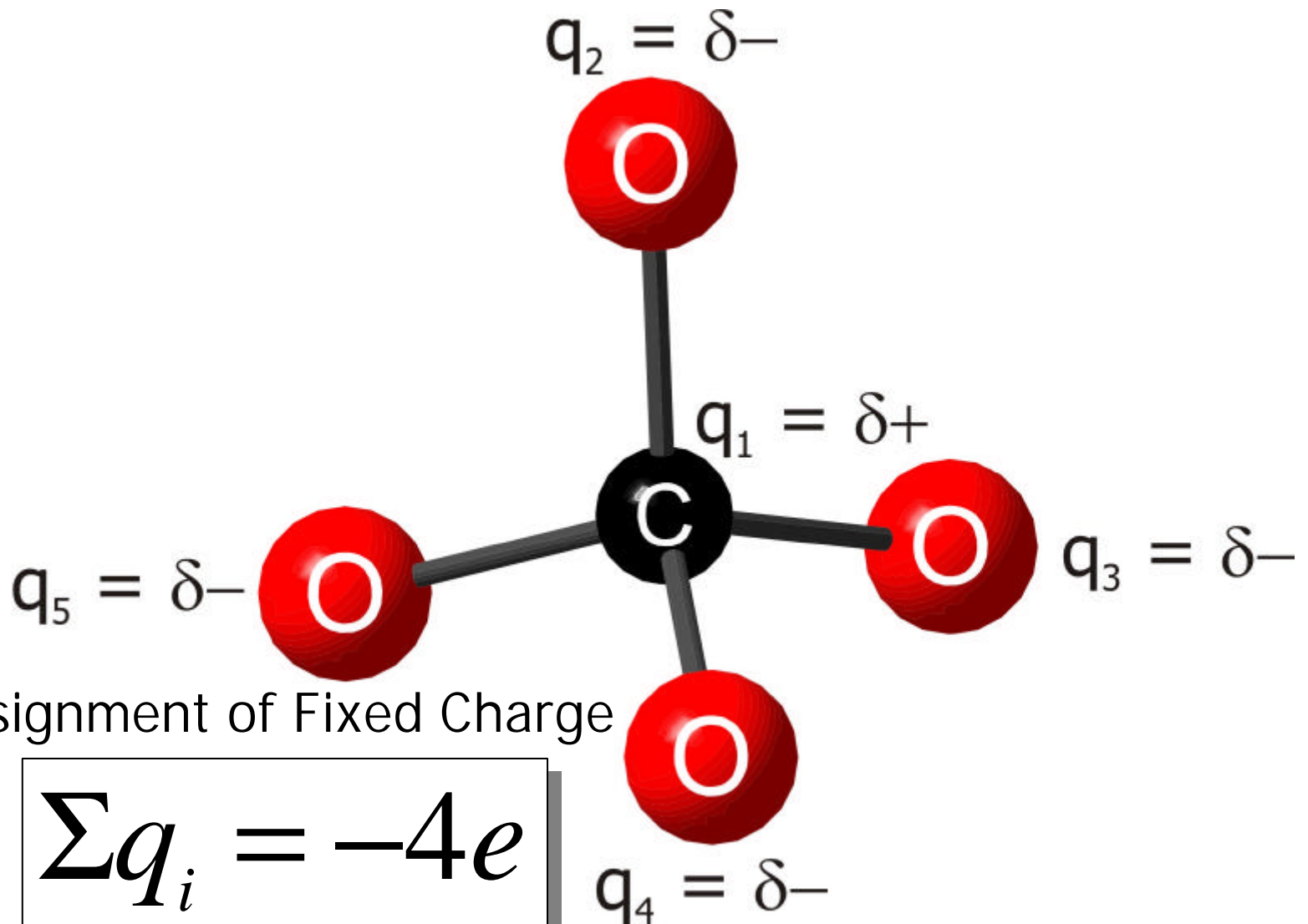


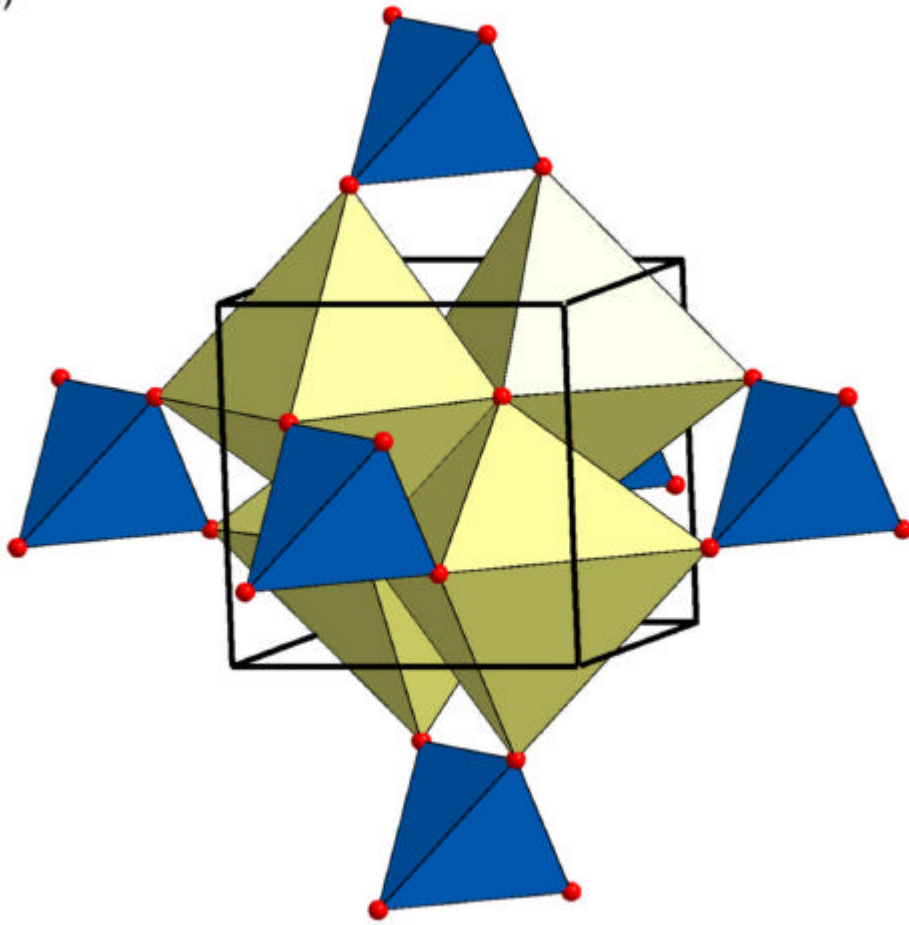
Figure 14:

Structure candidate, which was found during global optimizations of the MgCN_2 -system, using CN_2 -building units. The MgN_6 -octahedra form a distorted rutile structure. The space group of this (possibly high-pressure) structure candidate is $Pn\bar{m}$.

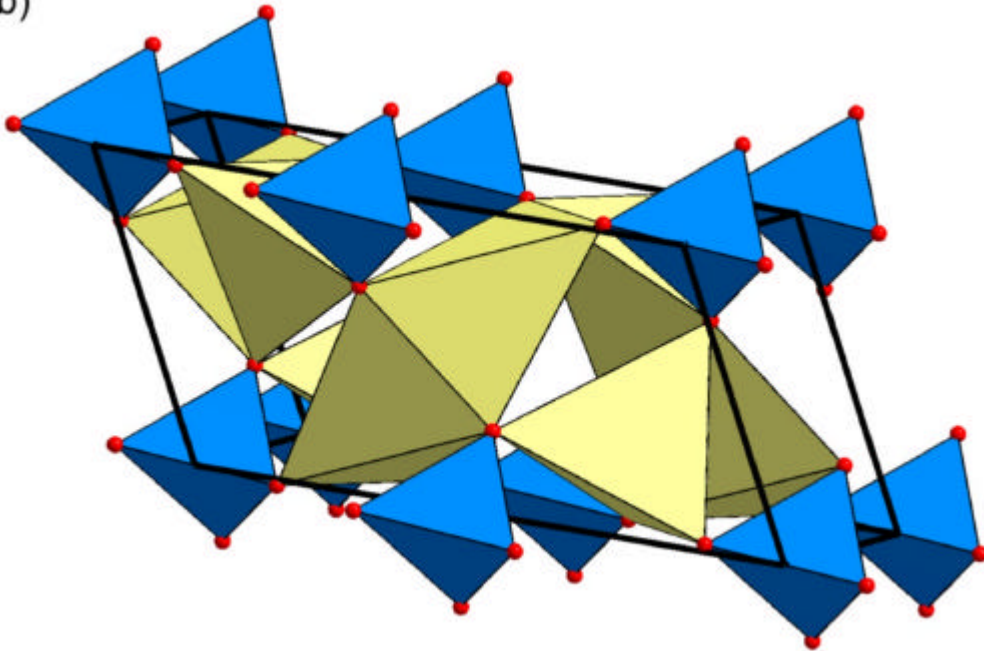
Movements of building units: Shift + Rotation + Exchange



a)



b)



Structure candidates found during global optimizations of the Li_4CO_4 -system, using CO_4 -building units. **a)** $\text{Li}_4(\text{CO}_4)$ -I: blue tetrahedra represent CO_4 -units, yellow octahedra represent LiO_6 -units; **b)** $\text{Li}_4(\text{CO}_4)$ -VI: blue tetrahedra represent CO_4 -units, yellow tetrahedra represent LiO_4 -units. Red balls represent oxygen atoms.

Comments

- Global search with building units (tetrahedral CO₄-units)
- For each global search, the charges, distances and angles within the building units were fixed
- Feedback-loop between global search and local optimization including fitting of bond-length within building unit according to local ab initio optimization until self-consistent results are reached.
- Prediction[20]: High-pressure ($p > 10$ GPa) structure candidates for Li₄CO₄ containing tetrahedral CO₄-units.

Structure determination

- Synthesis successful - structure unknown!
Often: Powder data ? Model

- Solution from powder data
 1. Extraction of cell parameters, cell content, intensities of reflexes
 2. Generation of structure model
(global optimization problem)
 3. (Rietveld)-Refinement via profile-fitting (local optimization)

- Commonly used: Patterson, direct methods, RMC, ...

Alternative: Pareto-Optimization[11]

- Minimization of energy and data
 $\implies C(\vec{r}_i) = \lambda_P E_{pot}(\vec{r}_i) + (1 - \lambda_P) R_B(\vec{r}_i)$
- Synergy:
 E_{pot}, I_{exp} need not be excellent
 \implies general simplified potentials employable
- Technical aspects
 - $\lambda_P \approx 1/2$
 - Input:
cell, cell content, intensities
 - Moveclass for simulated annealing
 - * Moving /exchanging atoms
 - * Optimization in $P1$
 - Speed (400 MHz Pentium):
 - * Na_3OCl : 1000 steps \approx 2 sec
 - * $In_2Ni_{21}B_6$: 2×10^6 steps \approx 2 weeks (116 atoms)

- Potential:

- a) $E_{pot} = \frac{1}{2} \sum_{i,j} \frac{e^2 q_i q_j}{4\pi\epsilon_0 d_{ij}} + \frac{A_{ij}}{d_{ij}^{12}} - \frac{B_{ij}}{d_{ij}^6}$
(ionic)

- b) $E_{pot} = E_0 + \frac{1}{2} \sum_{i,j} E_{ij}^{rep}$

$$E_{ij}^{rep} = \begin{cases} 0 & : d_{ij} \geq d_{ij}^{min} \\ \left(\frac{d_{ij}^{min}}{d_{ij}}\right)^6 - 1 & : d_{ij} < d_{ij}^{min} \end{cases}$$

(intermetallic, for good powder data)

- $R_B = 100 \frac{\sum_{2\theta} |I_{exp}(2\theta) - I_{ber}(2\theta)|}{\sum_{2\theta} I_{exp}(2\theta)}$

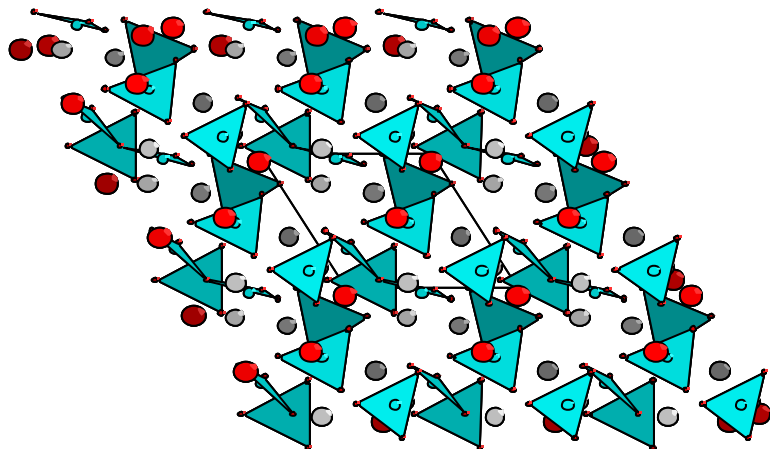
- $I_{ber}(hkl) = \frac{1}{N} LP |F(hkl)|^2$

(LP = polarisation factor)

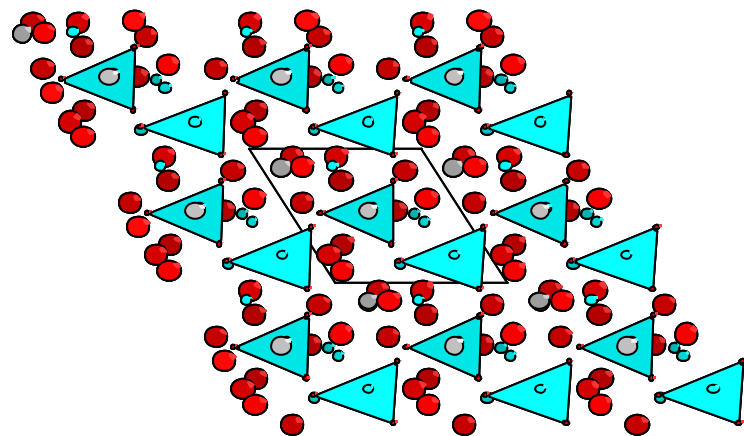
$$F(hkl) = \exp\left(-B \frac{\sin^2(\theta(hkl))}{\lambda^2}\right) \sum_j \left[f_j \exp(i\vec{h}\vec{r}_j) \right]$$

- $I_{ber}(2\theta) = \sum_{\theta \in [\theta, \theta + \Delta]} I_{ber}(hkl)$

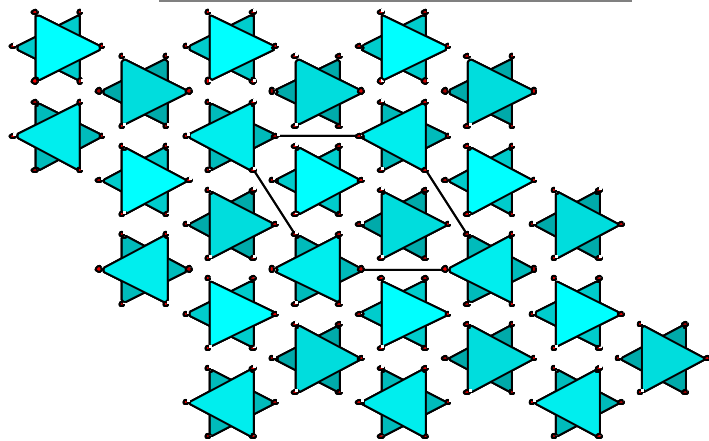
Pareto-optimization of CaCO_3 (30 atoms)



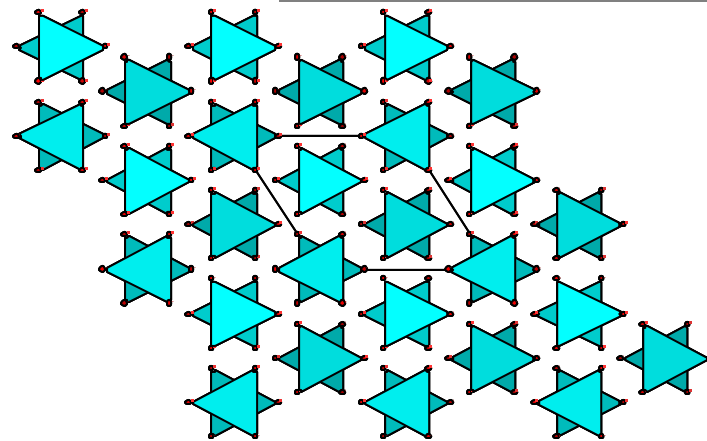
Only E_{pot}



Only R_B



Pareto



Calcite (Exp.)

Comments

- Demonstration example: CaCO_3 . Using only the simplified energy function or the powder diffraction information by itself is not sufficient (a high-level empirical potential using building units does find reasonable structure candidates). The combination of energy function and powder diffraction yields perfect agreement with experimental structure.

Examples

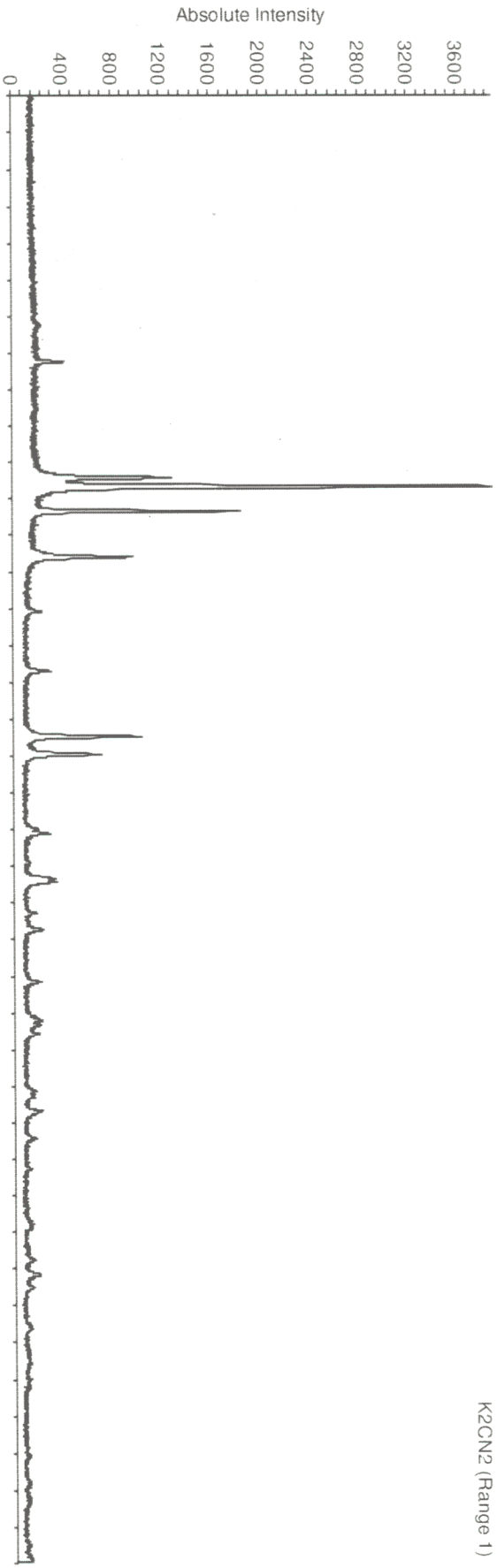
Compound	"Potential"	Powder data	Atom/cell
Na_3PS_4	ionic	exp.	16
$CaCO_3$ (Calcite)	ionic	exp.	30
$MgSiO_3$ (Enstatite)	ionic	ber.	80
Mg_2SiO_4 (Forsterite)	ionic	exp.	28
Na_3OCl	ionic	ber.	5
Na_3OBr	ionic	exp.	5
Al_2O_3	ionic	exp.	30
SiO_2 (quartz)	ionic	exp.	9
SiO_2 (cristobalite)	ionic	exp.	12
SiO_2 (stishovite)	ionic	exp.	6
TiO_2 (rutile)	ionic	exp.	6
TiO_2 (anatase)	ionic	exp.	12
TiO_2 (brookite)	ionic	exp.	24
MgO	ionic	exp.	8
MgF_2	ionic	exp.	6
CaF_2	ionic	exp.	12
$In_2Ni_{21}B_6$	metallic	exp.	116
In_2Ni_6B	metallic	exp.	36
$MgCu_2$	metallic	ber.	24
$MgZn_2$	metallic	exp.	12

Structure determinations

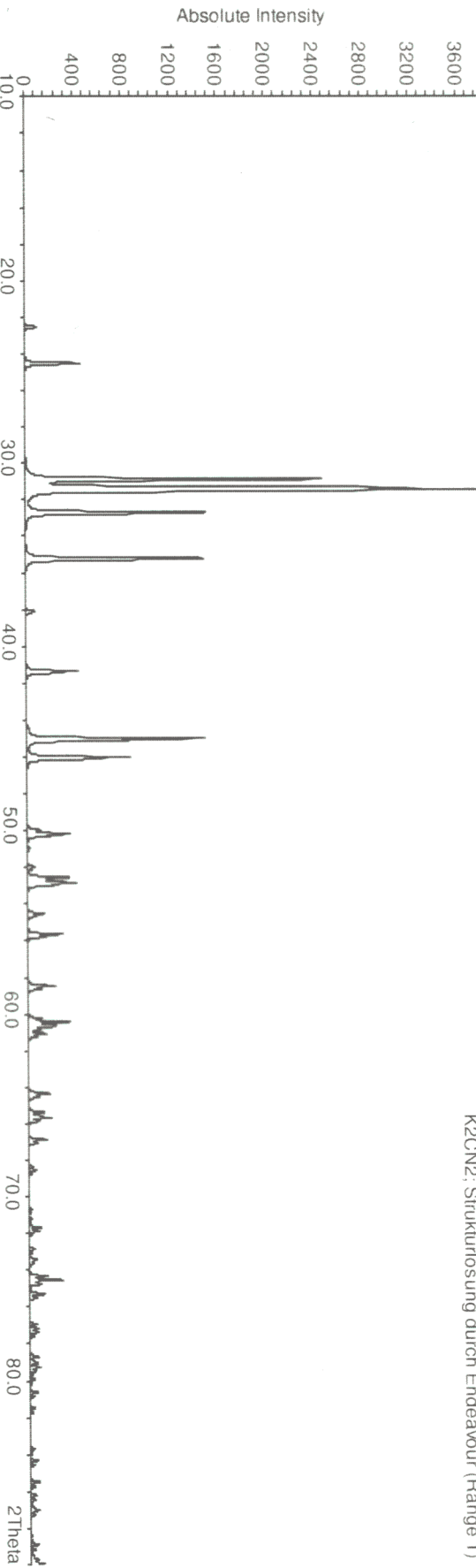
- $K_2(CN_2)[37]$
- $Na_3PSO_3[38]$

$K_2(CN)_2$

K2CN2 (Range 1)



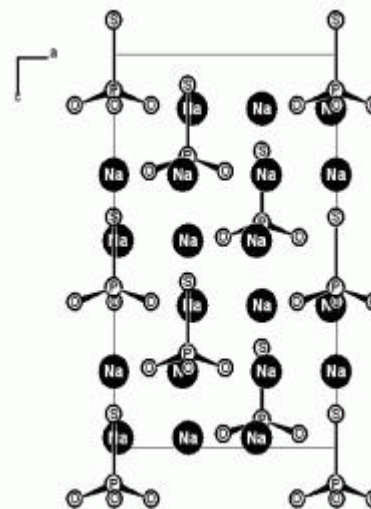
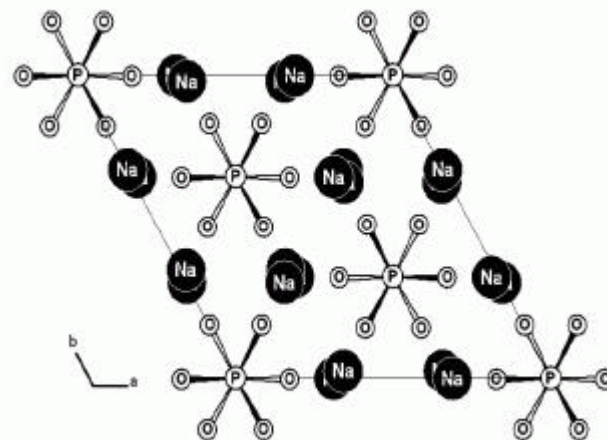
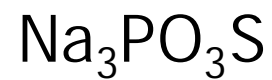
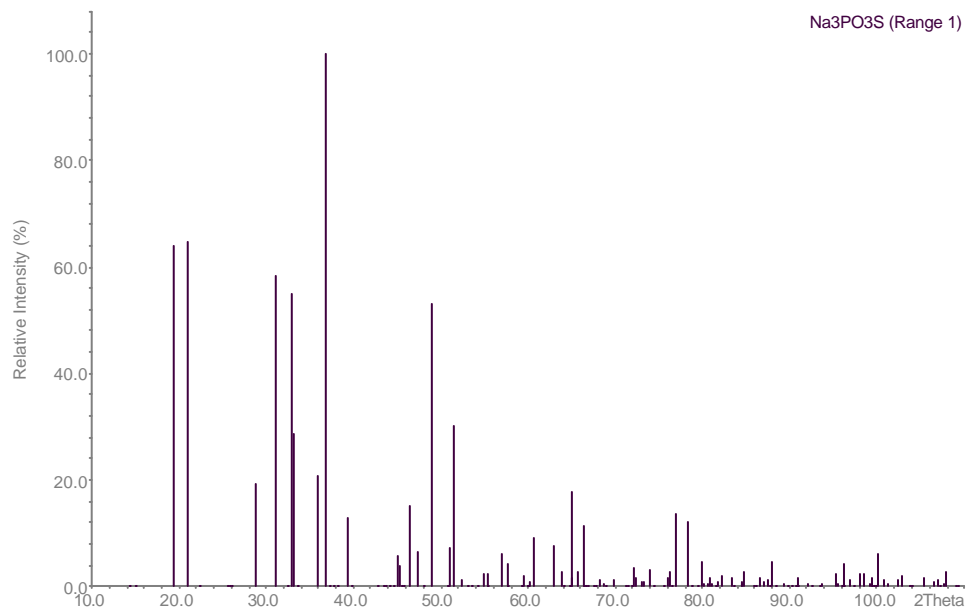
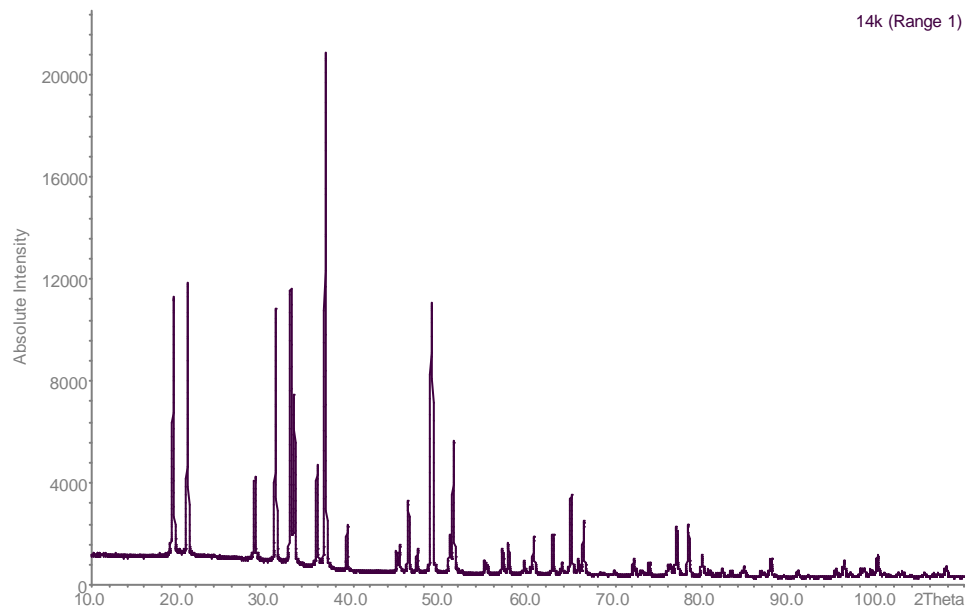
K2CN2: Strukturlösung durch Endeavour (Range 1)



M. Becker, M. Jansen

Comments

- Example[37]: Solving structure from powder data together with energy function for K_2CN_2 .
- Figure shows calculated and measured powder diffractogram.



Comments

- Example[38]: Solving structure from powder data together with energy function for $\text{Na}_3\text{PO}_3\text{S}$.
- Figure shows calculated and measured powder diffractogram, and structure of $\text{Na}_3\text{PO}_3\text{S}$.

Fields of application[2, 3]

- Clusters/molecules/polymers
Many structures; nice "test systems" for abstract theoretical methods; no periodicity; ab initio energy landscapes accessible
- Proteins
Secondary/tertiary structure; intensive data-mining (similarity arguments); primary building units on all scales; environment of protein important; general shape already success
- Molecular crystals
Packing of rigid/floppy molecules; primary building units; tiny energy differences between modifications (Problems: energy function, temperature/pressure dependence); limited data-mining (preferred space groups, number of molecules in unit cell)
- "Atom"-based solids
Type of bonding (empirical potential); ab initio programs needed for local optimization; influence of kinetics regarding outcome; no data-mining (except testing ICSD); primary building units possible; usually few problems with temperature/pressure
- "Building-unit"-based solids
Coordination polyhedra (secondary building units) on many scales; specially optimized potentials available as alternative to ab initio calculations; temperature/pressure influence excluded by construction
- Amorphous solids
No unique structure (many possible amorphous "structures", each with structural bandwidth and controlled by kinetics); No periodic (gigantic unit cells necessary - ab initio very expensive); need to simulate structure generation process

References

- [1] J. C. Schön and M. Jansen. A First Step towards Planning of Syntheses in Solid State Chemistry: Determination of Promising Structure Candidates using Global Optimization. *Angew. Chem. Int. Ed. Eng.*, 35:1286–1304, 1996.
- [2] J.C. Schön and M. Jansen. Determination, Prediction, and Understanding of Structures Using the Energy Landscape Approach - Part I. *Z. Krist.*, 216:307–325, 2001.
- [3] J. C. Schön and M. Jansen. Determination, prediction, and understanding of structures, using the energy landscapes of chemical systems - Part II. *Z. Krist.*, 216:361–383, 2001.
- [4] J. H. Holland. *Adaptation in Natural and Artificial Systems*. Univ. Mich. Press, Ann Arbor, 1975.
- [5] S. Kirkpatrick, C. D. Gelatt Jr., and M. P. Vecchi. Optimization by Simulated Annealing. *Science*, 220:671–680, 1983.
- [6] V. Czerny. Thermodynamic Approach to the Travelling Salesman Problem - an Efficient Simulation Algorithm. *J. Optim. Theo. Appl.*, 45:41–51, 1985.
- [7] D. A. Keen and R. L. McGreevy. Structural modeling of glasses using reverse Monte Carlo simulation. *Nature*, 344:423–425, 1990.
- [8] J. Pannetier, J. Bassas-Alsina, J. Rodriguez-Carvajal, and V. Caignaert. Prediction of crystal structures from crystal chemistry rules by simulated annealing. *Nature*, 346:343–345, 1990.
- [9] C. M. Freeman, J. M. Newsam, S. M. Levine, and C. R. A. Catlow. Inorganic Crystal Structure Prediction Using Simplified Potentials and Experimental Unit Cells - Application to the Polymorphs of Titanium-Dioxide. *J. Mater. Chem.*, 3:531–535, 1993.
- [10] M. W. Deem and J. M. Newsam. Determination of 4-connected framework crystal structures by simulated annealing. *Nature*, 342:260–262, 1989.
- [11] H. Putz, J. C. Schön, and M. Jansen. Combined Method for "Ab Initio" Structure Solution from Powder Diffraction Data. *J. Appl. Cryst.*, 32:864–870, 1999.
- [12] A. A. Coelho. Whole-profile structure solution from powder diffraction data using simulated annealing. *J. Appl. Cryst.*, 33:899–908, 2000.
- [13] O. J. Lanning, S. Habershon, K. D. M. Harris, R. L. Johnston, B. M. Kariuki, E. Tedesco, and G. W. Turner. Definition of a "guiding function" in global optimization: a hybrid approach combining energy and R-factor in structure solution from powder diffraction data. *Chem. Phys. Lett.*, 317:296–303, 2000.
- [14] A Y. Liu and M. L. Cohen. Structural properties and electronic structure of low-compressibility materials: β -Si₃N₄ and hypothetical β -C₃N₄. *Phys. Rev. B*, 41:10727–10734, 1990.
- [15] U. Müller. Vorhersage möglicher Kristallstrukturtypen mit Hilfe der kristallographischen Gruppentheorie. In H. Burzlaff, editor, *Proc. Symposium on predictability of crystal structures of inorganic solids*, pages 74–88. Friedrich-Alexander Universität Nürnberg, Nürnberg, 1997.
- [16] W. E. Klee, M. Bader, and G. Thimm. The 3-regular nets with four and six vertices per unit cell. *Z. Krist.*, 212:553–558, 1997.
- [17] J. C. Schön and M. Jansen. Determination of Candidate Structures for Simple Ionic Compounds through Cell Optimisation. *Comp. Mater. Sci.*, 4:43–58, 1995.
- [18] J. C. Schön and M. Jansen. Structure prediction of solids via investigation of potential energy surfaces. *Acta Cryst A (Suppl.)*, 55, 1999.

- [19] J. C. Schön and M. Jansen. Structure Prediction and Determination of Crystalline Compounds. In G. Meyer, D. Naumann, and L. Wesemann, editors, *Inorganic Chemistry Highlights*, pages 55–70. Wiley-VCh, Weinheim, 2002.
- [20] C. Mellot-Draznieks, S. Girard, G. Ferey, J. C. Schön, Z. Cancarevic, and M. Jansen. Computational Design and Prediction of Interesting Not-Yet-Synthesized Structures of Inorganic Materials using Building Unit Concepts. *Chem. Eur. J.*, 8:4102–4113, 2002.
- [21] C. Mellot Draznieks, J. M. Newsam, A. M. Gorman, C. M. Freeman, and G. Ferey. De Novo Prediction of Inorganic Structures Developed through Automated Assembly of Secondary Building Units (AASBU Method). *Angew. Chem. Int. Ed. Eng.*, 39:2270–2275, 2000.
- [22] M. A. C. Wevers, J. C. Schön, and M. Jansen. Global Aspects of the Energy Landscape of Metastable Crystal Structures in Ionic Compounds. *J. Phys.: Cond. Matt.*, 11:6487–6499, 1999.
- [23] J. C. Schön, M.A.C. Wevers, and M. Jansen. Characteristic regions on energy landscapes of complex systems. *J. Phys. A: Math. Gen.*, 34:4041–4052, 2001.
- [24] J. C. Schön, M. A. C. Wevers, and M. Jansen. Entropically stabilized region on the energy landscape of an ionic solid. *J. Phys.: Cond. Matter*, 15:5479–5486, 2003.
- [25] J. C. Schön. Studying the Energy Hypersurface of Multi-Minima Systems - the Threshold and the Lid Algorithm. *Ber. Bunsenges.*, 100:1388–1391, 1996.
- [26] J. C. Schön, H. Putz, and M. Jansen. Investigating the energy landscape of continuous systems - the threshold algorithm. *J. Phys.: Cond. Matt.*, 8:143–156, 1996.
- [27] Z. Cancarevic, J. C. Schön, and M. Jansen. Structure prediction of solids: Heuristic algorithms for local optimization on hartree-fock level. *Proc. Yucomat2003*, 2003.
- [28] H. Haas and M. Jansen. Li_4SeO_5 , the first orthoselenate, crystallizes as an order variant of a theoretically predicted $\text{A}^{[5]}\text{B}^{[5]}$ structure type. *Angew. Chem. Int. Ed. Eng.*, 38:1910–1911, 1999.
- [29] M. Jansen and J. C. Schön. Strukturkandidaten für Alkalimetallnitride. *Z. Anorg. Allg. Chem.*, 624:533–540, 1998.
- [30] D. Fischer and M. Jansen. Synthese und Struktur von Na_3N . *Angew. Chem. Int. Ed.*, 41:1755–1756, 2002.
- [31] D. Fischer, Z. Cancarevic, J. C. Schön, and M. Jansen. Zur Synthese und Struktur von K_3N . *Z. Allgem. Anorg. Chem.*, page accepted, 2003.
- [32] H. Putz, J. C. Schön, and M. Jansen. Structure Prediction for Crystalline Ca_3SiBr_2 using an Environment Dependent Potential. *Z. Anorg. Allg. Chem.*, 625:1624–1630, 1999.
- [33] Z. Cancarevic, J. C. Schön, and M. Jansen. *in preparation*, 2003.
- [34] A. Vegas, A. Grzechnik, K. Syassen, I. Loa, M. Hanfland, and M. Jansen. Reversible Transitions in Na_2S Under Pressure: A Comparison with the Cation Array in Na_2SO_4 . *Acta Cryst. B*, 57:151–156, 2001.
- [35] A. Grzechnik, A. Vegas, K. Syassen, I. Loa, M. Hanfland, and M. Jansen. Reversible Antifluorite to Anticotunnite Phase Transition in Li_2S at High Pressures. *J. Solid State Chem.*, page 603, 2000.
- [36] G. Bergerhoff, R. Hundt, R. Sievers, and I. D. Brown. The Inorganic Crystal Structure Database. *J. Chem. Inf. Comp. Sci.*, 23:66–69, 1983.
- [37] M. Becker and M. Jansen. Synthesis of Potassium Cyanamide, and Crystal Structure Determination by Pareto Optimization of the Cost Functions "Lattice Energy" and "Powder Intensities". *Sol. State Sci.*, 2:711–715, 2000.
- [38] M. Pompetzki and M. Jansen. Natriummonothiophosphat (V): Kristallstruktur und Natriumionenleitfähigkeit. *Z. anorg. allg. Chem.*, 628:641–646, 2002.